2009

Capillary electrophoretic separations of enzyme inhibitors with activity-based detection

Xiaoyan Yan
Louisiana State University and Agricultural and Mechanical College

CAPILLARY ELECTROPHORETIC SEPARATIONS OF ENZYME INHIBITORS WITH ACTIVITY-BASED DETECTION

A Thesis

Submitted to the Graduate Faculty of the
Louisiana State University and
Agricultural and Mechanical College
in partial fulfillment of the
requirements for the degree of
Master of Science

in

The Department of Chemistry

by
Xiaoyan Yan
B.S., Dalian University of Technology, Dalian, China, 2001
May 2009

ACKNOWLEDGEMENTS

I would first like to thank my advisor Dr. Gilman for his guidance. My thanks also go to everyone from the Gilman research group for once being my lab mates and making working in the lab comfortable. I also want to express my appreciation to all my friends for their friendship over the years. My deepest gratitude goes out to my parents, Ronghua Yan and Qiulan Ju, and my husband, Xiaodong Huang, for their unconditional love, continuous support and encouragement.

TABLE OF CONTENTS

LIST OF FIGURES

ABSTRACT

A technique for separating and detecting enzyme inhibitors was developed using capillary electrophoresis with an enzyme microreactor. The on-column enzyme microreactor was constructed using one or two NdFeB magnets in two configurations to immobilize alkaline phosphatase-coated superparamagnetic beads with diameters of 2.8 μm inside a capillary before the detection window. Enzyme inhibition assays were performed by injecting a plug of inhibitor into a capillary filled with an alkaline phosphatase substrate, AttoPhos. Product generated in the enzyme microreactor was detected by laser-induced fluorescence. Inhibitor zones electrophoresed through the capillary, passed through the enzyme microreactor, and were observed as negative peaks due to decreased product formation in the presence of the inhibitors.

The goal of this study was to improve peak capacities for inhibitor separations relative to previous work, which combined continuous engagement electrophoretically mediated microanalysis (EMMA) and transient engagement EMMA to study enzyme inhibition. The effects of electric field strength, bead injection time and inhibitor concentrations on peak capacity and peak width were investigated. Increasing the electric field strength from 100 V/cm to 500 V/cm caused a 2-3-fold decrease in peak capacity for alkaline phosphatase inhibition assays with arsenate, a reversible, competitive inhibitor. When the bead injection time was increased to increase the length of the immobilized bead plug, the peak capacity for arsenate reached a minimum value at 60.0 s for the one-magnet configuration and at 30.0 s for the two-magnet configuration. The peak capacity was enhanced to 20 under optimal conditions of electric field strength and bead injection time for inhibition assays with arsenate and theophylline. The inhibition peak width increased as the concentrations of arsenate and theophylline increased. Five reversible inhibitors of alkaline phosphatase (theophylline, orthovanadate, arsenate, L-tryptophan and tungstate) were separated and detected to demonstrate the ability of this

technique to analyze complex inhibitor mixtures. A well-resolved, individual inhibition peak was observed for each inhibitor. Enzyme inhibition assays with a mixture of the five inhibitors were also performed with the previous EMMA method, and a peak capacity of only 3 was obtained (all 5 inhibitors could not be resolved).

CHAPTER 1
INTRODUCTION

1.1 Enzyme Assays

Enzymes are biological catalysts for chemical reactions in all living systems. Like other chemical catalysts, enzymes increase the reaction rate by lowering the activation energy [1-7]. Protein-based enzymes are the dominant form of biocatalyst. Also, there are a few RNA molecules called ribozymes that catalyze fundamental biochemical reactions [1, 4]. Enzymes are responsible for enabling the many chemical processes that are taking place at any time in a biological cell. Enzyme catalysis has been used by people for thousands of years for fermentation in both bread and alcohol production [3, 4]. Enzyme catalysis is now widely used for commercial applications. Enzymes are used to prepare fabrics in the textile industry and to tan hides in the leather industry [4, 8-10]. Enzymes are used as ingredients in detergents [4, 8, 11], and have also found various applications in the pulp and paper industry [8, 12]. In addition, they play an important role in the production of biofuel from crops such as sugar cane and corn [8, 13]. Since enzymes are highly efficient catalysts that work under mild conditions of temperature, pH and pressure and are also enantiospecific, they are employed to catalyze the syntheses of organic compounds [3, 14]. Moreover, enzymes are the biologically responsive material in many biosensors [15, 16].

Enzymes have an active site, where the reacting molecule, called the substrate, binds and where the chemical reaction occurs. The active site is usually a small pocket on the enzyme surface, which contains the binding and catalytic functional groups. The structural and chemical properties of the active site make the enzyme specific for only one type of substrate [1, 3-5, 7]. The general scheme for an enzyme-catalyzed reaction is:

$$E + S \underset{k_{-1}}{\overset{k_1}{\rightleftharpoons}} ES \xrightarrow{k_2} E + P$$

In an enzyme-catalyzed reaction, the substrate (S) binds to the active site of the enzyme (E) to form an intermediate complex (ES), which proceeds to form product (P) or dissociates back to enzyme (E) and substrate (S). With the product (P) being formed, free enzyme (E) molecule is released and the catalytic cycle begins again [1, 3-7].

A quantitative analysis of enzyme-catalyzed reactions was proposed by Henri (1903) and by Michaelis and Menten (1913) [4, 5, 7]. They assumed that $k_2 << k_{-1}$ in the general reaction scheme. In the Henri–Michaelis–Menten model, the reversible step between E + S and the ES complex reaches equilibrium very rapidly, and the ES complex converts slowly to product (P). A more sophisticated and general model was later developed by Briggs and Haldane (1925) based on the steady-state approximation [4, 5, 7]. This model does not assume $k_2 << k_{-1}$ and states that a steady state arises shortly after the beginning of the enzyme-catalyzed reaction. During the period of steady state, the rate of formation of the ES complex is equal to the sum of the rate of its dissociation back to substrate (S) and the rate of its transformation to product (P). Therefore, the ES concentration is constant. From the steady-state approximation the following rate equation, which describes the dependence of the reaction velocity on the substrate concentration, can be derived:

$$v = \frac{V_{\max}[S]}{K_{\mathrm{m}} + [S]} \qquad (1.1)$$

This is the basic equation of enzyme kinetics. In honor of the pioneering work of Henri, Michaelis and Menten, this equation is commonly referred to as the Michaelis–Menten or Henri–Michaelis–Menten equation [1-7]. The Michaelis constant, K_m, is the ratio of the elementary rate constants.

$$K_m = \frac{k_{-1} + k_2}{k_1} \tag{1.2}$$

K_m represents the substrate concentration at which the reaction velocity is half of the maximal velocity, V_{max}. The Michaelis–Menten plot is depicted in Figure 1.1. From Figure 1.1, it can be noted that at low [*S*], substrate availability limits the reaction rate, and thus the reaction velocity, *v*, increases proportionally with [*S*]. At much higher [*S*], the reaction velocity, *v*, reaches V_{max}. At V_{max} all enzyme molecules have substrate bound to them. Adding more substrate will not increase the reaction rate. This situation is called substrate saturation.

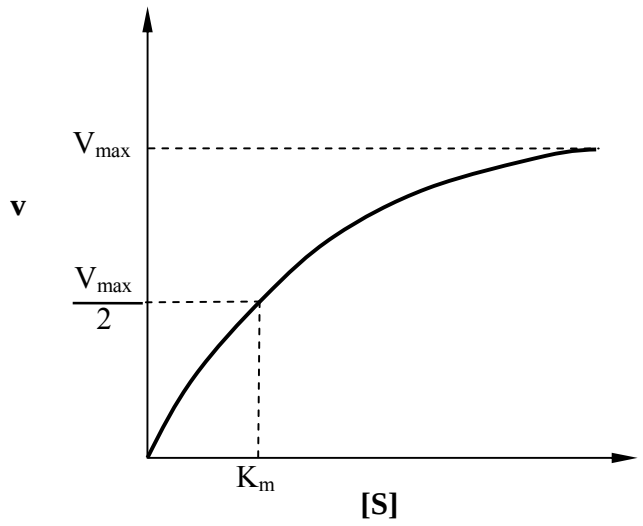

Figure 1.1. Michaelis–Menten plot

By taking the reciprocal of both sides of Equation 1.1, the Michaelis–Menten equation can be transformed into

$$\frac{1}{v} = \frac{1}{V_{\max}} + \left[\frac{K_{\mathrm{m}}}{V_{\max}}\right]\frac{1}{[S]} \tag{1.3}$$

According to Equation 1.3, a plot of 1/*v* versus 1/[*S*] yields a straight line with a slope of K_m/V_{max} and an intercept of $1/V_{max}$, as illustrated in Figure 1.2. A plot like that in Figure 1.2 is known as a

Lineweaver–Burk plot. By fitting the experimental data linearly in a Lineweaver–Burk plot, the kinetic constants K_m and V_{max} can be determined from the slope and the intercept, respectively [1, 3-7].

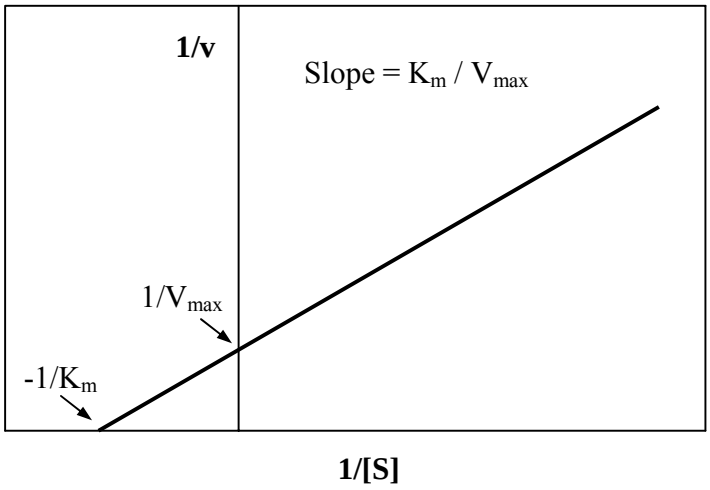

Figure 1.2. Lineweaver–Burk plot

Enzyme assays are experimental measurements of enzyme activity. In order to generate a Michaelis–Menten plot and a Lineweaver–Burk plot for the determination of two important parameters in enzyme kinetics, K_m and V_{max}, enzyme assays are performed by measuring the velocity of an enzyme-catalyzed reaction at varying substrate concentrations. The reaction velocity is determined by monitoring product formation or substrate depletion as a function of time [2, 4, 6]. Reaction progress curves similar to those illustrated in Figure 1.3 can be observed. The reaction velocity can be calculated as the slope of the initial linear portion of the reaction progress curves.

$$v = -\frac{d[S]}{dt} = \frac{d[P]}{dt} \tag{1.4}$$

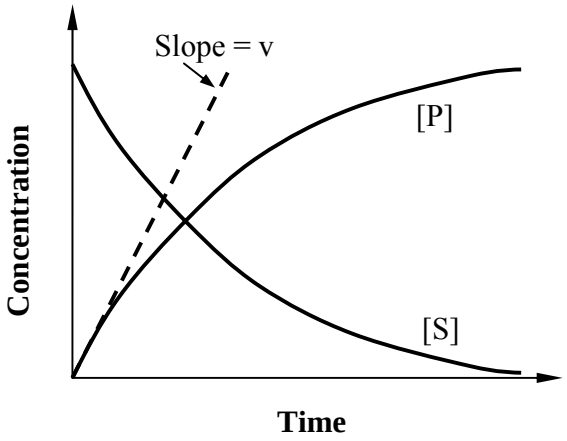

Figure 1.3. Reaction progress curves

In a typical enzyme assay, all but one of the required components for the enzyme-catalyzed reaction are added to the reaction vessel. This mixture of components is then equilibrated under certain conditions of pH, temperature, and ionic strength. Afterwards, the reaction is started by adding a small volume of a concentrated stock solution of the missing component, which can be the enzyme or the substrate, and by mixing the reaction mixture rapidly right after the addition. The initiating component is added as a small volume so that the experimental conditions of the reaction mixture do not change significantly [2, 4].

Detection in enzyme assays relies on a unique property of the substrate or product. Sometimes the substrate and product need to be separated before detection. Separation and detection methods that have been applied for enzyme assays include HPLC, gel electrophoresis, absorbance, fluorescence, radiochemical and electrochemical techniques. In direct assays, the substrate or product concentration can be measured directly as a function of time. When the substrate and product do not provide a distinct signal, indirect assays are carried out by coupling the enzyme-catalyzed reaction to another enzymatic or nonenzymatic reaction to produce a convenient signal for detection [2, 4].

1.2 Enzyme Assays Based on Capillary Electrophoresis (CE)

Capillary electrophoresis (CE) has emerged as a powerful separation tool. With the application of an electric field, CE separates compounds based on their differential mobilities, which depend upon the charge, size and shape of the individual compounds as well as the viscosity of the electrophoresis buffer [17, 18]. Capillary electrophoresis has been successfully applied for the study of enzyme assays [19-25]. Compared to traditional enzyme assay methods, CE has several significant advantages. The amount of sample used in CE is extremely small due to the small dimensions of capillaries and microfabricated devices. Capillary electrophoresis is capable of separating the reaction products from the substrates with high efficiency. Capillary electrophoresis also offers high-speed analysis compared to other separation techniques. Furthermore, CE can be used in conjunction with several detection methods, such as UV-vis spectrometry, laser-induced fluorescence (LIF), mass spectrometry (MS), and electrochemical detection (EC). In addition, CE has excellent quantitation capabilities for studying enzyme assays [19-25].

Capillary electrophoresis was initially used only as a separation tool in the determination of enzyme activities, and the enzyme-catalyzed reactions were performed off-line [20, 21]. In off-line enzyme assays, all components of an enzyme-catalyzed reaction are first mixed outside the capillary and incubated for a period of time. Then, the reaction mixture is injected into the capillary for separation of the substrate and product. Although off-line CE-based enzyme assays offer some advantages such as highly efficient separation and high sensitivity, it has limitations. The enzyme-catalyzed reaction and sample analysis do not occur at the same time. Before injection of the reaction mixture into the capillary, the reaction must be completely stopped by using some methods to denature the enzyme or by rapidly freezing the reaction solution.

Although the sample volume needed for CE analysis is only a few nanoliters, much larger volumes of reaction components are needed to carry out the reaction. In order to shorten the delay period between the time of reaction and the time of analysis and to reduce the consumption of reaction reagents, the reaction should be conducted on-line, inside the capillary [20, 21].

On-line enzyme assays in CE can be classified into two categories: heterogeneous assays and homogeneous assays [20, 23, 25]. In a heterogeneous enzyme assay, either the enzyme or the substrate (most often the enzyme) is immobilized inside the capillary or the channel on a microchip to create an enzyme microreactor. The enzyme-catalyzed reaction takes place between the immobilized reaction component and the free solution component. The resultant product is directly transported to the end of the capillary and then detected. Heterogeneous enzyme assays have several advantages. The stability of the immobilized enzyme often is enhanced compared to the enzyme in free solution. Enzyme microreactors also can be reused conveniently. The enzyme immobilized on a solid support can be easily separated from the substrate and product. However, enzyme activity may be changed due to immobilization. Also, the preparation procedure of an enzyme microreactor can be complicated and time-consuming [20, 23, 25, 26].

In a homogeneous enzyme assay inside the capillary or on a microchip, the enzyme-catalyzed reaction occurs with all reaction components including the enzyme and the substrate in the buffer solution [20-23, 25]. Unlike in heterogeneous assays, the enzyme in homogeneous assays remains in solution. Therefore, enzyme kinetic studies performed by homogeneous CE assays can produce results similar to those obtained with traditional assays. One problematic issue in homogeneous assays is that the enzyme can adsorb undesirably to the capillary wall or the channel surface in a microchip.

The first on-line homogeneous enzyme assay in CE was described by Bao and Regnier in 1992 [27]. The capillary was first filled with the substrate (S) and also the required coenzyme (Figure 1.4a). Then, a plug of the enzyme (E) was injected into the capillary (Figure 1.4b). As the enzyme migrated through the capillary by electrophoresis, it interacted with the substrate to form the enzyme-substrate complex (ES) and produce the product (P) (Figure 1.4c), which was detected at a downstream absorbance detector (Figure 1.4d). This type of assay, based on an enzyme-catalyzed reaction carried out electrophoretically in a capillary column, was later termed electrophoretically mediated microananlysis (EMMA), and this specific format was defined as continuous engagement EMMA [21-25]. The typical procedure for carrying out enzyme assays using continuous engagement EMMA is depicted in Figure 1.4. In continuous engagement EMMA, a product plateau is formed since the product is produced from the continuous interaction between the substrate and the migrating enzyme plug. In order to increase product formation, the applied high voltage can be turned off for incubation. With this zero-potential incubation, a product peak is observed on top of the plateau.

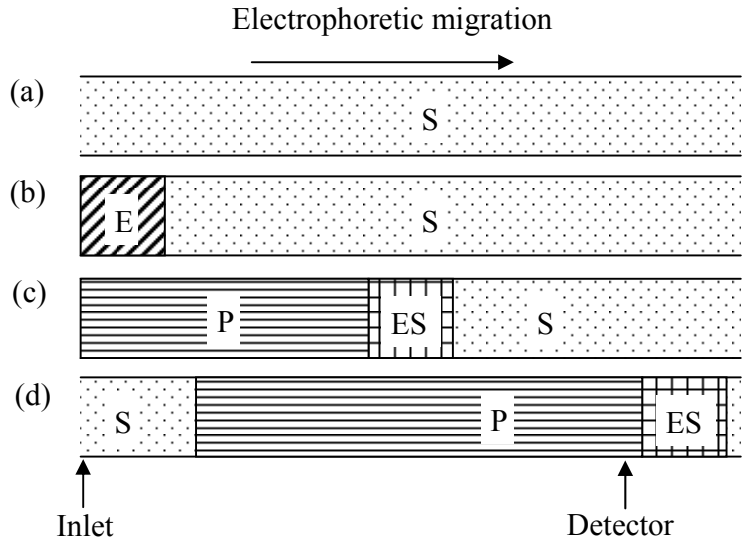

Figure 1.4. Continuous engagement EMMA. (a) A capillary filled with substrate. (b) Injection of enzyme. (c) Formation of product. (d) Detection of product.

The second type of EMMA is transient engagement EMMA, which is also called plug-plug mode EMMA. In transient engagement EMMA (Figure 1.5), the enzyme (E) and the substrate (S) are injected into the capillary as separate plugs, with the reaction component with lower electrophoretic mobility injected first (Figure 1.5a). Upon the application of an electric field, these two plugs merge (Figure 1.5b-c) and then separate from each other (Figure 1.5d) due to differences in their electrophoretic mobilities. During the time period when the two plugs are overlapped, the enzyme-catalyzed reaction takes place and the enzyme-substrate complex (ES) is formed to generate product (P) in the capillary (Figure 1.5b-c). The reaction components are later detected downstream as separate peaks (Figure 1.5d) [21-25].

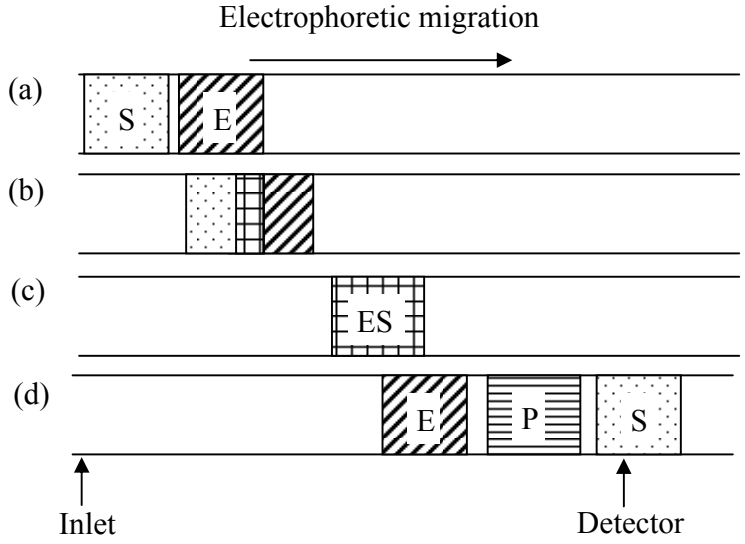

Figure 1.5. Transient engagement EMMA. (a) Injection of enzyme and substrate. (b) Start of overlap between two plugs. (c) Full overlap. (d) Separation and detection of substrate and product.

Electrophoretically mediated microananlysis (EMMA) has been applied in many enzymatic systems to carry out enzyme activity assays, determine Michaelis constants (K_m) for enzyme kinetic studies and study enzyme inhibition [21, 23, 28]. β-Galactosidase assays were performed on microchip by Burke and Regnier using continuous engagement EMMA with laser-induced fluorescence (LIF) detection [29], and in capillary by Kanie et al. using transient engagement

EMMA with UV detection [30]. Jin et al. reported the determination of zeptomole amounts of glucose-6-phosphate dehydrogenase in human erythrocytes and the measurement of alkaline phosphatase isoenzymes in individual fibroblast cells of mouse bone marrow by a combination of zero-potential incubation in capillary and electrochemical detection (EC) [31, 32]. Hoogmartens et al. described a kinetic study of phenol sulfotransferase SULT1A1 by CE-UV and determined its K_m value [33]. The use of EMMA in enzyme inhibition studies will be discussed in Section 1.4.

1.3 Enzyme Inhibition

Enzyme inhibitors are molecules that reduce the rate of an enzyme-catalyzed reaction by binding to the enzyme molecule [1-7]. Enzyme inhibitors can decrease the activity of specific enzymes, and they are used commercially as herbicides[34, 35] and pesticides [36, 37]. Many diseases are caused by dysregulated enzyme activity or by infectious organisms such as viruses and bacteria. Enzyme inhibitors, e.g. aspirin and captopril, are used as drugs to kill a pathogen or to modulate metabolic pathways in patients. Enzyme inhibitors have been central to the drug discovery and development process [7, 38]. Moreover, a better understanding of the mechanism of enzyme catalysis can be gained from enzyme inhibition studies [1, 4, 7].

Enzyme inhibitors bind to the enzyme either reversibly or irreversibly. The bonding between a reversible inhibitor and the enzyme is nonconvalent, and the enzyme-inhibitor complex dissociates rapidly. The dissociation constant for the enzyme-inhibitor complex, K_i, is a measure of the affinity between the inhibitor and the enzyme.

$$\mathrm{E} + \mathrm{I} \rightleftharpoons \mathrm{EI}$$

$$K_i = \frac{[E][I]}{[EI]} \tag{1.5}$$

K_i is defined as the inhibition constant in reversible inhibition. It is commonly used to describe the potency of an inhibitor [1, 3-7].

There are three types of reversible inhibitors: competitive, noncompetitive, and uncompetitive inhibitors. They are classified according to how the inhibitor interactions with enzyme affect the equilibrium in an enzyme-catalyzed reaction. The Lineweaver–Burk plot can be used to illustrate the effect of the three types of reversible inhibition (Figure 1.6a-c) [1, 3-7].

In competitive inhibition, the inhibitor usually resembles the structure of the substrate, and it competes with the substrate for binding to the active site on the enzyme. The bindings of the inhibitor and the substrate are mutually exclusive, and the inhibitor only binds to the free enzyme molecule. The maximal velocity V_{max} is not affected by competitive inhibition. Both the Michaelis constant K_m and also the slope in Lineweaver–Burk plot K_m/V_{max} are increased (Figure 1.6a) [1, 3-7].

In noncompetitive inhibition, the inhibitor binds to a site different from the enzyme's active site. The inhibitor and the substrate can bind simultaneously to an enzyme molecule. The substrate binds to E and EI, and the inhibitor binds to E and ES; however, the created ESI cannot form product. When the affinity of the inhibitor for the free enzyme and the ES complex are equivalent, a Lineweaver–Burk plot like the one in Figure 1.6b is generated, in which the lines converge at the *x*-axis. When the inhibitor binds with greater affinity to the free enzyme, the lines intersect above the *x*-axis; when the inhibitor has preferential affinity for the ES complex, the lines intersect below the *x*-axis. For all situations of noncompetitive inhibition, V_{max} is decreased and K_m/V_{max} is increased (Figure 1.6b) [3-7].

In uncompetitive inhibition, the inhibitor also binds to a site on the enzyme other than the active site. The inhibitor has no affinity for the free enzyme and binds only to the ES complex.

The resulting ESI is a dead end complex, and cannot form product. Both K_m and V_{max} are decreased equally in the presence of an uncompetitive inhibitor, and thus the slope K_m/V_{max} is constant while the *y*-intercept increases (Figure 1.6c) [3-7].

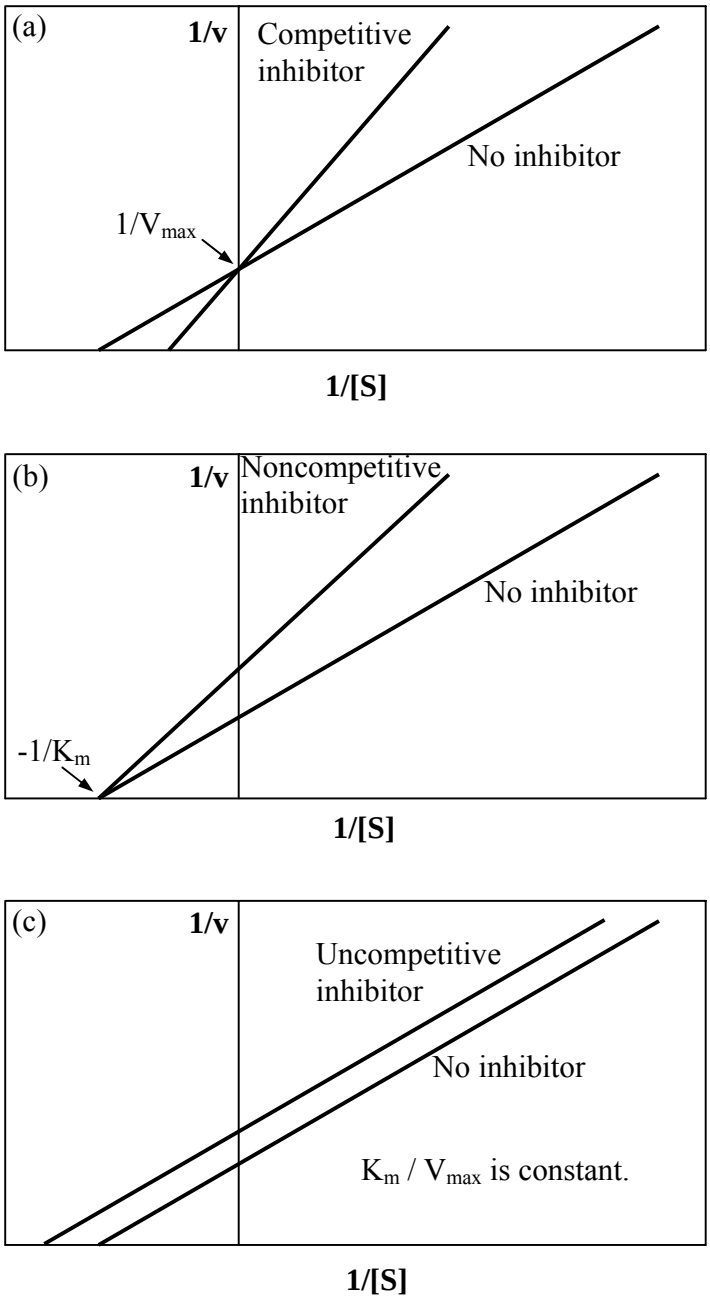

Figure 1.6. Lineweaver–Burk plots for reversible inhibition

Unlike reversible inhibitors that dissociate from the enzyme, an irreversible inhibitor forms covalent bond with the enzyme molecule and does not dissociate. The enzyme is permanently inactivated due to the irreversible interaction between the inhibitor and enzyme. Therefore, irreversible inhibitors are also known as enzyme inactivators. Since the formation of covalent bonds is relatively slow, irreversible inhibitors display time dependency. The degree of inhibition increases with time after the irreversible inhibitor interacts with the enzyme [3-7].

1.4 On-line Enzyme Inhibition Assays Based on CE

On-line enzyme assays in CE have been employed to study enzyme inhibition [28]. Heterogeneous enzyme inhibition assays based on CE have been reported in which enzymes are immobilized onto a capillary or a microfabricated device [39-41]. Tang and Kang described inhibition assays of angiotensin-converting enzyme (ACE) in an on-column microreator, which was created by an ionic binding technique [40]. The capillary was first coated with hexadimethrine bromide (HDB). A short plug of enzyme was then incubated with the positively charged HDB and was immobilized on inlet part of the capillary wall via ionic bonding. After flushing the capillary with the running buffer, enzyme inhibition assays were carried out by hydrodymanically injecting a mixture of the inhibitor and the substrate hippuryl-His-Leu (HHL). After incubation of the substrate with the immobilized enzyme, an electric field was applied to separate the substrate HHL and the product hippuric acid (HA), which were then detected by UV absorbance. Captopril and cilazaprilat were investigated in the inhibition assays, and were confirmed as competitive and noncompetitive ACE inhibitors, respectively.

Enzyme assays based on continuous engagement EMMA have also been applied to study enzyme inhibition [42, 43]. Using continuous engagement EMMA, Belenky and coworkers investigate the inhibition of protein tyrosine phosphatase [42]. The inhibitor sample was added to

the substrate solution, and this mixture was used to fill the capillary. After the enzyme was injected and migrated for some time in the capillary, the voltage was turned off for zero-potential incubation. Inhibition assays were performed using this method to screen inhibitors of protein tyrosine phosphatase in a natural extract. Hadd et al. used continuous engagement EMMA to study the inhibition of β-galactosidase on a microchip device [43]. The substrate, buffer, enzyme, and inhibitor were held in separate reservoirs and mixed electrophoretically. The substrate and the buffer were first mixed in the upstream channel. The enzyme and the inhibitor were then added to the diluted substrate solution at a cross intersection to carry out the enzyme-catalyzed reaction in the downstream channel. The generated product was fluorescent and was detected by a downstream laser-induced fluorescence (LIF) detector. The inhibition of β-galactosidase by three inhibitors, phenylethyl β-D-thiogalactoside (PETG), *p*-hydroxymercuribenzoic acid (PHMB) and D-lactose was investigated.

In addition, enzyme inhibition assays using transient engagement EMMA have been reported [44-48]. The inhibition of adenosine deaminase by erythro-9-(2-hydroxy-3-nonyl)adenine (EHNA) was studied by Saevels et al. using the traditional mode of transient engagement EMMA as illustrated in Figure 1.5 [44]. The inhibitor, EHNA, was added to the running buffer, the enzyme solution and also the substrate solution to carry out the enzyme inhibition assays. The Glatz research group employed the partial filling technique, a modification of transient engagement EMMA, to perform inhibition studies of rhodanese and haloalkane dehalogenase [45-47]. The partial filling technique was first introduced by Van Dyck et al., and offers the advantage of using different buffer systems for carrying out the enzyme-catalyzed reaction and separating the reaction components [49]. Using the partial filling technique, the Glatz research group studied the inhibition of rhodanese by 2-oxoglutarate [45]. The capillary was filled with β-

alanine buffer at pH 3.5 for CE separation. The enzyme and a mixture of the substrate and inhibitor were prepared in HEPES buffer at pH 8.5, which is optimal for the enzyme-catalyzed reaction, and were then injected into the capillary subsequently as distinct zones. In order to shield the reaction component plugs from the separation buffer and to provide a suitable environment for the reaction to take place, a plug of HEPES buffer at pH 8.5 was injected before the enzyme zone and also after the substrate and inhibitor zone. The K_i values of 2-oxoglutarate with respect to each substrate, thiosulfate and cyanide, were determined. This laboratory later used the same technique to investigate the inhibition of haloalkane dehalogenase by a competitive inhibitor 1,2-dichloroethane and the substrate inhibition of this enzyme by 1,2-dibromoethane [46, 47].

Whisnant et al. in our lab used a combination of continuous engagement EMMA and transient engagement EMMA to study the inhibition of alkaline phosphatase [50, 51]. The capillary was first filled with a solution of the fluorogenic substrate, AttoPhos (2'-[2-benzothiazoyl]-6'-hydroxybenzothiazole phosphate), which would be converted to a fluorescent product by the catalysis of alkaline phosphatase. Then, the inhibitor and enzyme were injected electrokinetically into the capillary as separate plugs, with the inhibitor being injected first since it has a lower electrophoretic mobility compared with the enzyme-substrate complex. After this, a constant high voltage was applied to carry out the inhibition assay. As the enzyme-substrate complex migrated through the capillary under the electric field, the fluorescent product was generated continuously, which was observed as a plateau by a downstream laser-induced fluorescence (LIF) detector (Figure 1.7). Moreover, the zones of inhibitor and enzyme-substrate complex mixed electrophoretically as the faster moving enzyme-substrate complex zone overtook the slower moving inhibitor zone. During this overlap time, the enzyme-catalyzed

reaction slowed down due to the inhibition, resulting in formation of less product. For a reversible inhibitor, the enzyme activity was restored after the zones of inhibitor and enzyme-substrate complex were separated from each other. A negative inhibition peak was observed on the product plateau as shown in Figure 1.7. The inhibition types and K_i values of three reversible inhibitors, theophylline, sodium vanadate and sodium arsenate, were determined. In addition, the authors also demonstrated the use of this method to investigate the irreversible inhibition of alkaline phosphatase by EDTA.

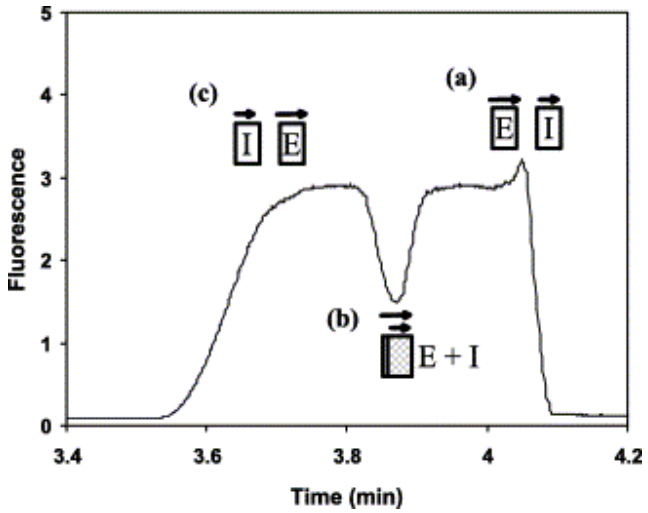

Figure 1.7. Electropherogram of a theophylline-alkaline phosphatase enzyme-inhibitor assay (Figure from Reference 51)

Compared to traditional enzyme assays in microplates, this CE-based technique requires significantly less enzyme. Using this on-line EMMA method, reversible inhibition and irreversible inhibition can be easily distinguished based on the shape of electropherograms. It is capable of quantifying competitive and noncompetitive reversible inhibitors using Michaelis–Menten treatment of the data and determining K_i values for these inhibitors.

This CE-based enzyme inhibition assay is not suitable for the separation of mixtures of enzyme inhibitors since it has a very low peak capacity. The peak capacity (n_c) is the maximum

number of separated peaks that can fit into the path length or space provided by the separation method with adjacent peaks at a specified resolution (R_s) value [17]. The peak capacity is a figure of merit for quantifying the ability of a separation method to resolve complex mixtures, and can be calculated from the following equation for adjacent peaks separated at $R_s = 1$,

$$n_c = \frac{L}{w}, \tag{1.6}$$

where L is the total path length or space of separation, and w is the peak width. In the enzyme inhibition assays developed by Whisnant et al. [50, 51], the space for separation of mixtures of enzyme inhibitors is the width of the plateau, and the peak width is the width of the negative inhibition peak at the baseline. As can be seen in Figure 1.7, L is about 21 s, and w is about 6 s. Therefore, n_c is about 3, which means that at most three inhibitors can be separated by using this method. This value of the peak capacity is not high enough for the purpose of separating a mixture of enzyme inhibitors.

This thesis presents the development of a new approach for enhancing the peak capacity for enzyme inhibitor separations using on-line enzyme inhibition assays based on CE. To perform the enzyme assays and separate enzyme inhibitors, an on-column enzyme microreactor was constructed by coating the magnetic beads with alkaline phosphatase and holding the magnetic beads in place by a magnet at the downstream part of the capillary. Enzyme inhibitors were separated in capillary before they reached the immobilized enzyme. Individual inhibitors moved downstream, passed the enzyme zone, and were detected as negative peaks. Using this approach, separations of five inhibitors of alkaline phosphatase (theophylline, sodium orthovanadate, sodium arsenate, L-tryptophan and sodium tungstate) were demonstrated.

CHAPTER 2
CAPILLARY ELETROPHORETIC SEPARATIONS OF ENZYME INHIBITORS WITH ACTIVITY-BASED DETECTION

2.1 Introduction

Because enzyme catalysis plays a central role in biological chemistry, enzymes are one of the most important classes of drug targets, and enzyme inhibitors have been central to the drug discovery and development process [7]. Rapid, inexpensive and information-rich analytical techniques are needed for enzyme inhibitor screening [7]. When potential enzyme inhibitors are part of a synthetic or natural mixture of compounds, it would be desirable to use analysis methods that simultaneously separate compounds in the mixture and examine their inhibition of a target enzyme.

Capillary electrophoresis (CE) has been successfully applied for studies of enzyme kinetics and enzyme inhibition in both capillaries and microchips [23, 28]. Whisnant et al. developed a method combining continuous engagement EMMA and transient engagement EMMA to study the inhibition of alkaline phosphatase in a capillary [50, 51]. In principle, this EMMA method could be used to perform inhibitor separations together with enzyme inhibition assays; however, poor peak capacity limits this approach in practice. For example, the peak capacity based on studies of the reversible inhibition of alkaline phosphatase by theophylline is calculated to be 3 [51]. In 1999, Hadd et al. reported an EMMA-based method in a microchip device, which could separate mixtures of inhibitors and detect them based on their inhibition of the target enzyme [52]. Four inhibitors of acetylcholinesterase, tetramethylammonium chloride, tetraethylammonium chloride, tacrine and edrophonium, were separated and detected as negative peaks due to reduced product formation. Despite the promise of this early study, no subsequent reports appeared in the literature applying this approach or further developing it.

Described here is a simple, on-column CE method in a capillary for separating mixtures of inhibitors and detecting these molecules based on their inhibition of a target enzyme. To overcome the limited peak capacity of the EMMA method developed by Whisnant and coworkers [50, 51], the enzyme was immobilized in the CE capillary before the detector by immobilizing enzyme-coated paramagnetic beads with a magnetic field [53]. The enzyme inhibitors were separated by CE before reaching the enzyme microreactor. The effects of several experimental variables on the assays, such as bead injection time and separation potential, were investigated. Five reversible inhibitors of alkaline phosphatase were separated, and their individual inhibition peaks were observed using this approach. This method was directly compared to the EMMA method reported by Whisnant et al. [50, 51] using the same enzyme and mixture of inhibitors.

2.2 Materials and Methods

2.2.1 Reagents

Alkaline phosphatase (EC 3.1.3.1 from calf intestine) and AttoPhos (2´-[2-benzothiazoyl]-6´-hydroxybenzothiazole phosphate) were obtained from Promega (Madison, WI). Sodium phosphate and sodium hydroxide were purchased from Fisher Scientific (Fair Lawn, NJ). Sodium vanadate was from Acros Organics (Pittsburgh, PA). Other chemicals were supplied by Sigma-Aldrich (St. Louis, MO). All solutions were prepared in ultrapure water (> 18 MΩ·cm) from a Modulab water purification system (United States Filter Corp.; Palm Desert, CA).

2.2.2 CE-LIF Instrumentation

The CE-LIF instrument was constructed in house and is similar to previous instruments [50, 51]. Figure 2.1 shows a schematic representation of the instrument. The LIF detector is not shown in detail. The 457.9-nm line of an air-cooled argon ion laser (543R-AP-A01, Melles Griot;

Carlsbad, CA) was used for excitation. The laser beam was focused onto the capillary by a CaF_2 plano convex lens (f = 20.0 mm) (Thorlabs; Newton, NJ). The laser power at the capillary was 24.0 mW. The fluorescence was collected at 90° relative to the excitation beam by a 20× microscope objective (0.5 NA; Melles Griot; Carlsbad, CA), and was filtered by a 560 ± 10 nm bandpass filter (53900, Oriel; Stratford, CT) and an 800 μm diameter pinhole (Oriel). The fluorescence was then detected by a PMT (HC120-01, Hamamatsu; Bridgewater, NJ) at a potential of 1000 V. The PMT output was filtered by a low-pass filter at 50 Hz, and the data were collected at 20 Hz by the data acquisition board (PCI-6229, National Instruments; Austin, TX). A LabVIEW program (Version 7.1, National Instruments) was written and used for data acquisition. The data were analyzed using OriginLab 7.5 (Northampton, MA).

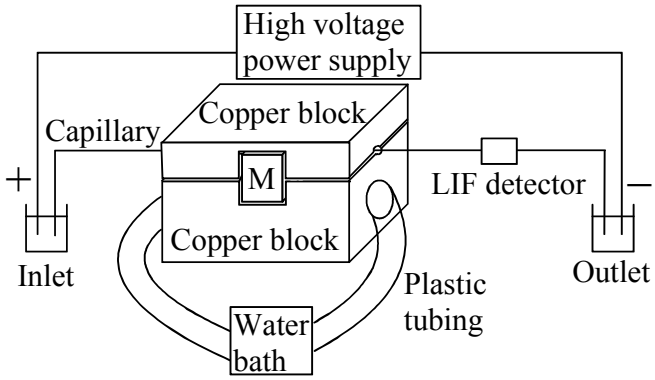

Figure 2.1. Diagram of the CE-LIF instrument. The copper block was used to hold the magnet (M) in place and to thermostat the capillary in the region where the enzyme-coated magnetic beads were immobilized.

A Spellman CZE1000R high-voltage power supply (Hauppauge, NY) was used to apply the electrophoretic potential. Fused silica capillaries with a 50 μm i.d. and 220 μm o.d. from SGE (Austin, TX) were used. For all experiments, the capillaries were 60.0 cm total length and 45.0 cm to the detection window. The detection window was made by removing the polyimide

coating using a window maker (MicroSolv Technology; Eatontown, NJ). Each new capillary was rinsed before use with 0.1 M NaOH, water, and then diethanolamine (DEA) buffer (50.00 mM, pH 9.50) using a manual syringe pump for 10 min, respectively. All solutions used for CE were filtered through a 0.2-μm membrane filter (Whatman; Hillsboro, OR).

2.2.3 Enzyme Immobilization on Magnetic Beads

Superparamagnetic polystyrene beads (Dynabeads M-270 Epoxy) with diameters of 2.8 μm were purchased from Invitrogen Dynal (Olso, Norway). The covalent attachment of alkaline phosphatase to the magnetic beads was performed using the protocol provided by the manufacturer. Briefly, a batch of magnetic beads (1.5 mg, 1.0×10^8 beads) was washed twice with 100 μL of 100.0 mM sodium phosphate buffer at pH 7.40. In each washing step, the beads were separated from the wash buffer by immobilizing the bead suspension with a NdFeB magnet and removing the supernatant. The washed beads were then resuspended in 30 μL of the sodium phosphate buffer (3.3×10^9 beads/mL). After mixing the 30-μLsuspension of washed beads and 30 μL of 14 μM alkaline phosphatase in the same phosphate buffer, 30 μL of 3.000 M ammonium sulfate in the pH 7.40 phosphate buffer was added to enhance binding of alkaline phosphatase to the beads. The resultant mixture was incubated with slow tilt rotation on a rocking platform for 24 h at room temperature. After incubation, the beads were washed four times with 150 μL aliquots of DEA buffer (50.00 mM, pH 9.50) to remove alkaline phosphatase molecules that were not covalently attached to the beads. Finally, the beads were resuspended in 200 μL DEA buffer (5.0×10^8 beads/mL) and stored in the refrigerator at 4 °C until use. The coated bead suspensions were diluted to a concentration of 1.7×10^8 beads/mL, and the suspension was homogenized with a vortex mixer before injection into the CE capillary.

2.2.4 Magnetic Bead Immobilization in the Capillary

A copper holder was constructed to hold the magnets that immobilized the magnetic beads inside the capillary and to control the temperature in this region of the capillary. This holder is illustrated in Figure 2.1. The holder positioned the magnet(s) near the capillary surface, 27.0 cm from injection end of the capillary. Water from a thermostatted bath was circulated through the copper holder to control the temperature of a 5.0-cm section of the capillary, centered at the magnet. Permanent NdFeB magnets (B442 and D24) used in this work were purchased from K&J Magnetics (Jamison, PA). A B442 magnet (3700 Gauss) was secured in the holder with one pole perpendicular to the capillary bore. The distance from the center of the capillary bore to the face of the magnet closest to the capillary was 350 μm. In a 2-magnet configuration, a pair of D24 magnets (3895 Gauss) was secured in the holder. The two magnets were arranged at ±20° relative to the longitudinal axis of the capillary bore with their north poles facing the capillary bore [54]. The distance from the inner edge of each magnet to the center of the capillary bore was 395 μm. To create an enzyme microreactor with magnetic beads, the beads coated with alkaline phosphatase were electrokinetically injected into the capillary at 300 V/cm and then transported to the immobilization zone by electrophoresis (200 V/cm) in DEA buffer (50.00 mM, pH 9.50). After experiments, the beads could be easily removed by rinsing the capillary with DEA buffer using a manual syringe pump.

An inverted microscope (Nikon ECLIPSE TE 300) was used with a 10× objective to image immobilized magnetic beads inside the capillary. Images for the 1-magnet configuration were captured by a CCD camera and an imaging software (WinView Software Version 32) from Princeton Instruments (Trenton, NJ). A digital camera (Sony DSC-W55/P; Sony Electronics, Inc.) was used for the 2-magnet configuration to capture images of bead plugs observed through the

eyepiece diopter of the microscope. The bead plug lengths were measured using the inner diameter of the capillary (50 μm) as a reference.

2.2.5 Enzyme Assays

For heterogeneous enzyme assays in a capillary with immobilized magnetic beads, the running buffer was 0.100 mM AttoPhos in 50.00 mM DEA at pH 9.50. AttoPhos is a fluorogenic substrate for alkaline phosphatase. All inhibitor solutions were prepared in the running buffer. Inhibitors were electrokinetically injected at 200 V/cm for 3.0 s. The applied electric field for carrying out the enzyme assays was 200 V/cm unless otherwise noted. The electrode and the capillary inlet were dipped in DEA buffer before and after each injection of inhibitor to prevent cross contamination of the running buffer and inhibitor solution. The capillary was thermostatted at 25.0 °C. To analyze the data for heterogeneous enzyme inhibition assays, peak capacity (n_c) was calculated from the following equation

$$n_c = 0.5887 \frac{t}{w_{1/2}} \tag{2.1}$$

where t is the migration time of an inhibitor, and $w_{1/2}$ is the full width at half maximum of an inhibition peak [17].

For homogeneous CE enzyme inhibition assays, the basic experimental procedures were the same as those described previously [51]. The capillary was filled with the same running buffer used for the heterogeneous enzyme inhibition assay, including substrate. A zone of an alkaline phosphatase inhibitor, theophylline, was first injected for 3.0 s at 12.0 kV into the capillary. A potential of 12.0 kV was then applied for 30.0 s (40.0 s when a mixture of inhibitors was injected). Next, a plug of 51 pM alkaline phosphatase was injected for 3.0 s at 12.0 kV. Finally, a separation potential of 12.0 kV (200 V/cm) was applied. The enzyme concentration for homogeneous assays was obtained by injecting incubation mixtures of AttoPhos with the enzyme

in DEA buffer or the enzyme immobilized on magnetic beads and then comparing their product fluorescence signals. The inhibitor solutions contained the inhibitor as well as 0.100 mM AttoPhos in 50.00 mM DEA at pH 9.50. The electrode and the capillary inlet were dipped in DEA buffer before and after each injection to prevent cross contamination of the running buffer, enzyme solution and inhibitor solution. The thermostatting system for the homogeneous assays was constructed as described previously [51]. To thermostat the capillary, Teflon tubing was used to enclose the capillary from the injection end to the detection window, and N_2 (25.0 °C, 8 psi) flowed through the Teflon tubing around the capillary. The temperature of the N_2 was controlled by passing it through a coil of tubing in a temperature-controlled water bath before it passed over the capillary to control the capillary temperature.

2.3 Results and Discussion

2.3.1 Enzyme Microreactors for Enzyme Inhibition Assays

The goal for this work was to expand the ability of our CE enzyme inhibition assays to separate and detect mixtures of inhibitors [50, 51]. The approach presented here is to immobilize the enzyme of interest inside the capillary before the detector. The running buffer contains a fluorogenic substrate for the target enzyme – AttoPhos and alkaline phosphatase in this work. Inhibitor mixtures will separate by CE before reaching the enzyme microreactor, and they will produce a negative inhibition peak (reduced fluorescent product formation) as they migrate through the enzyme microreactor and inhibit the enzyme. Chetwyn and Susan Lunte used a related approach to separate and detect mixtures of acetylcholinesterase inhibitors based on an enzyme-modified electrode placed at the end of a CE capillary [55]. In the work presented here, the fluorescent reaction product is detected by LIF downstream from the enzyme microreactor.

The enzyme microreactors were constructed using rare earth magnets to immobilize enzyme-coated magnetic beads inside the capillary before the detection window [53]. Two different magnet configurations were used in this work. In both configurations, the magnets were placed 27.0 cm from injection end of the capillary. In the one-magnet configuration, a single B442 magnet (3700 Gauss) was placed with the face of the square magnet 350 μm from the center of the capillary bore with its pole facing the capillary bore. In the two-magnet configuration, two D24 magnets (3895 Gauss) were positioned at ±20° relative to the long axis of the capillary with their north poles facing the capillary [54]. The distance from the center of the capillary bore to the inner edge of each magnet was 395 μm. In both configurations, the magnets were able to hold magnetic beads in place inside capillary at the field strengths used in this study.

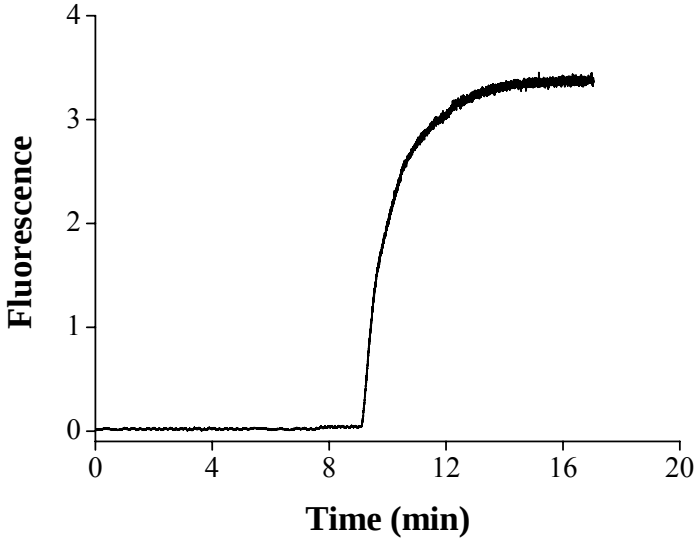

Figure 2.2. Electropherogram showing fluorescence without and with alkaline phosphatase substrate, Attophos, in the running buffer with an enzyme microreactor. A single B442 magnet (3700 Gauss) was used to immobilize magnetic beads inside capillary. Magnetic beads (1.7×10^8 beads/mL) coated with alkaline phosphatase in DEA buffer (50.00 mM, pH 9.50) were injected for 30.0 s at 18.0 kV (300 V/cm). Next, a potential of 12.0 kV (200 V/cm) was applied to the capillary filled with DEA buffer to transport the beads to the immobilizing magnet. Then the capillary was filled electrokinetically with substrate buffer containing 0.100 mM AttoPhos (50.00 mM DEA, pH 9.50) using an applied potential of 12.0 kV.

The use of magnetic immobilization of enzyme-labeled beads greatly simplified the development and optimization of this approach to CE-based enzyme inhibition assays. Enzyme microreactors could be constructed simply by electrokinetically injecting enzyme-coated magnetic beads into a capillary and then transporting the beads to the immobilizing magnet by electrophoresis in DEA buffer. No modification of the inner capillary surface was required. Figure 2.2 shows the increase in fluorescence when the DEA buffer used for immobilization (without substrate) is replaced with DEA buffer containing the substrate, AttoPhos.

2.3.2 Optimization of the Enzyme Assay

The temperature at the enzyme microreactor and the concentration of substrate in the running buffer were optimized before beginning enzyme inhibition studies. A 5.0 cm section of the capillary centered at the magnet was temperature controlled by circulating water from a thermostatted bath through the copper holder. The optimum temperature (maximum enzyme activity) was found to be 25 °C using the one-magnet configuration for immobilizing the alkaline phosphatase-coated magnetic beads. The data are presented in Figure 2.3. Although the temperature of the capillary was controlled externally at 25 °C, it is important to note that the temperature in the bore of the capillary will be higher than this due to Joule heating [56]. The electrophoretic current for this experiment was 3.9 μA.

The substrate concentration was optimized by measuring the fluorescence signal when buffers with AttoPhos concentrations ranging from 0.005 to 0.500 mM were allowed to electrophorese through the capillary at 200 V/cm. The fluorescence signal due to product formation at each AttoPhos concentration was recorded when it became stable. Figure 2.4 shows the fluorescence vs. substrate concentration, and K_m was determined to be 0.026 mM by fitting

the experimental data nonlinearly to the Michaelis–Menten equation. An AttoPhos concentration of 0.100 mM was used for subsequent experiments.

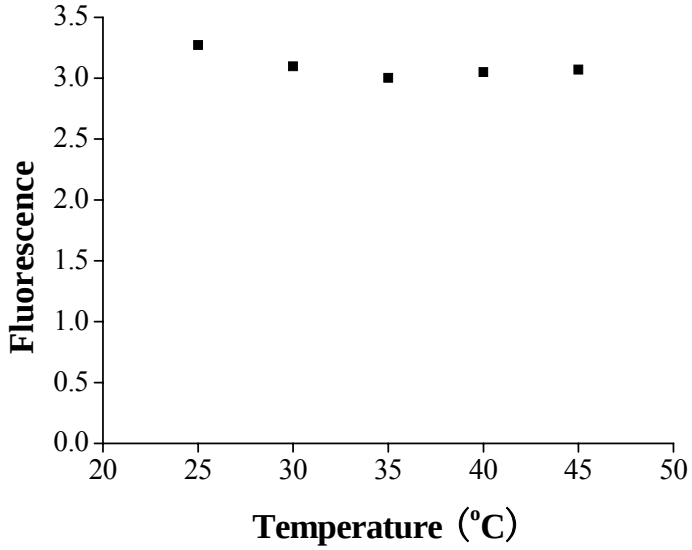

Figure 2.3. Fluorescence vs. external temperature at the enzyme microreactor for CE assays of alkaline phosphatase. Experimental conditions are the same as in Figure 2.2.

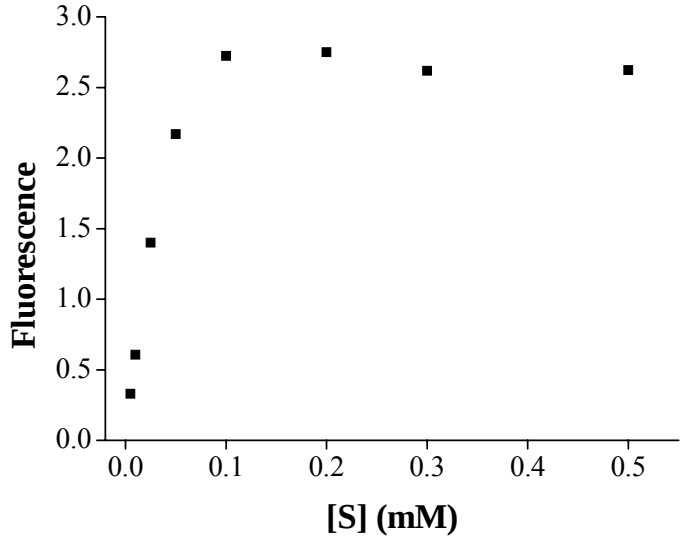

Figure 2.4. Plot of product fluorescence vs. substrate concentration. Experimental conditions are the same as in Figure 2.2.

2.3.3 Inhibition Assays

An electropherogram of an enzyme inhibition assay for sodium arsenate, a reversible competitive inhibitor of alkaline phosphatase, is presented in Figure 2.5. The enzyme microreactor was constructed using a single magnet. The enzyme microreactor first was filled with a 0.100 mM AttoPhos solution to obtain a constant fluorescence signal from the enzyme-catalyzed reaction product. Then, 0.125 mM sodium arsenate was injected for 3.0 s at 12.0 kV. Finally, a separation potential of 12.0 kV was applied. At 11.2 min, a decrease in product formation was observed due to the inhibitor zone passing through the plug of enzyme-coated magnetic particles. After the inhibitor zone migrated past the plug of beads, the product fluorescence returned to its original level and the enzyme activity was restored, demonstrating that sodium arsenate is a reversible inhibitor.

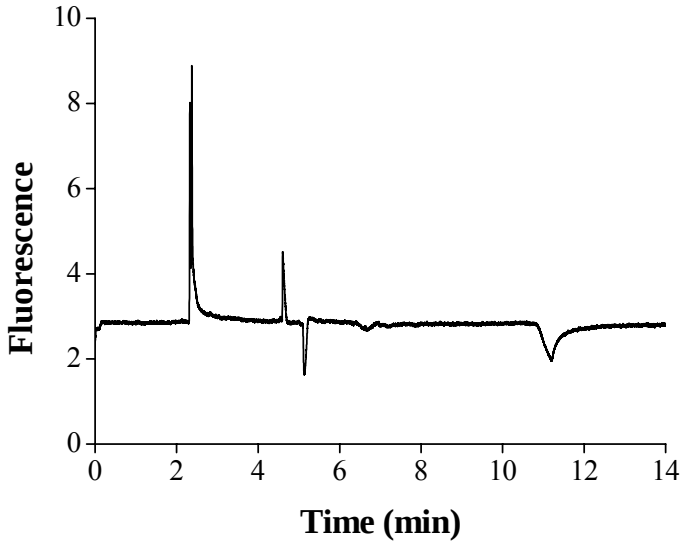

Figure 2.5. Electropherogram of an enzyme inhibition assay (inhibition of alkaline phosphatase by arsenate) using an enzyme microreactor constructed with a single magnet. Experimental conditions for loading the magnetic beads are the same as in Figure 2.2, and the same running buffer and substrate concentration were used. The inhibitor, 0.125 mM sodium arsenate, was injected for 3.0 s at 12.0 kV. Finally, a separation potential of 12.0 kV was applied.

The electropherogram also contains several artifact peaks. The unresolved peaks at ~2.3 min result from product formation during zero-potential incubation. The first peak was generated after the high voltage was turned off just before the inhibitor was injected into the capillary, and the second peak was generated after the inhibitor injection and before the application of the separation potential. There are also two reproducible artifact peaks (a positive peak and a negative peak) at ~4.9 min, and the cause of these two peaks is unclear. Electropherograms for the same experiments carried out in an enzyme microreactor constructed with two magnets (Figure 2.6) are similar in appearance to those obtained using a single magnet.

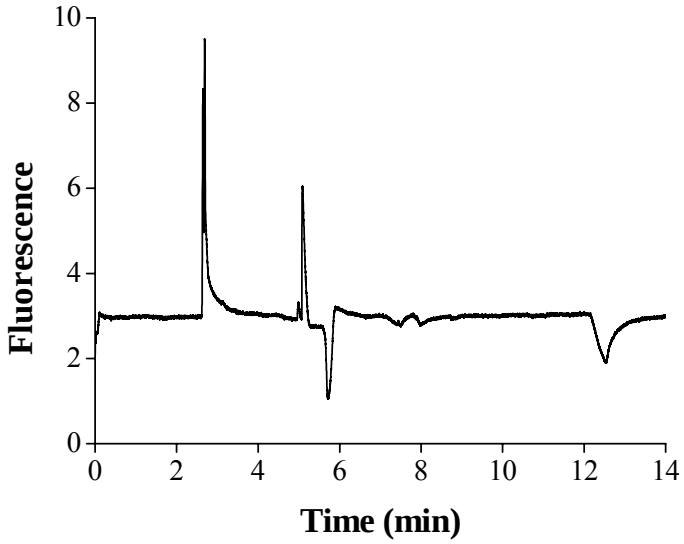

Figure 2.6. Electropherogram of an enzyme inhibition assay (inhibition of alkaline phosphatase by arsenate) using an enzyme microreactor constructed with two magnets. Experimental conditions are the same as in Figure 2.5.

The inhibition of alkaline phosphatase by theophylline was also studied with both enzyme microreactors. Theophylline is a reversible, noncompetitive inhibitor of alkaline phosphatase. An electropherogram for a 3.0-s injection of 1.00 mM theophylline is shown in Figure 2.7. The

negative peak at 8.4 min is due to theophylline inhibition. The artifact peaks are almost identical to those observed for arsenate.

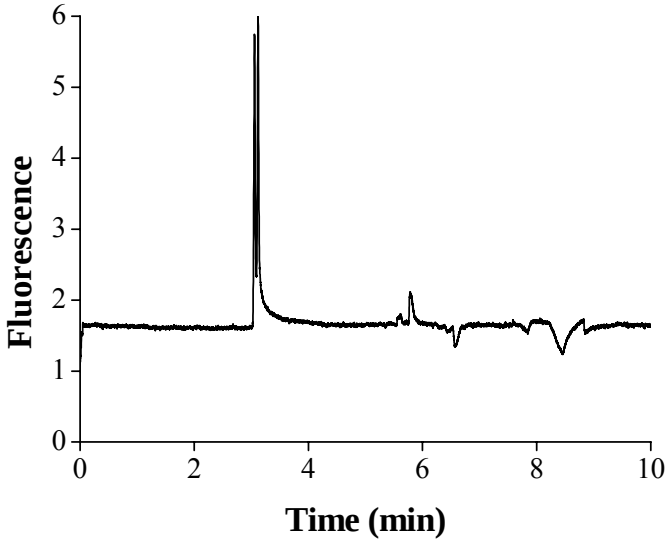

Figure 2.7. Electropherogram of an enzyme inhibition assay (inhibition of alkaline phosphatase by theophylline) using an enzyme microreactor constructed with a single magnet. The inhibitor, 1.00 mM theophylline, was injected for 3.0 s at 12.0 kV, and then the separation potential of 12.0 kV was applied. Magnetic beads (1.7×10^8 beads/mL) were injected for 15.0 s at 18.0 kV. All other experimental conditions are the same as in Figure 2.5.

2.3.4 Effects of Electric Field Strength and Bead Injection Time on Peak Capacity

The effects of the electric field strength and bead injection time on the peak capacity (n_c) for separation of reversible inhibitors were investigated to optimize the ability of the enzyme inhibition assays to resolve mixtures of inhibitors. Inhibition assays of alkaline phosphatase by arsenate were performed at different electric field strengths using enzyme microreactors constructed with one and two magnets. A plot of the peak capacity vs. field strength is presented in Figure 2.8. For both types of enzyme microreactors, the peak capacity decreases with increased electric field strength. Taking into consideration both the peak capacity and the total analysis time, an electric field strength of 200 V/cm was chosen for later experiments ($n_c \approx 20$).

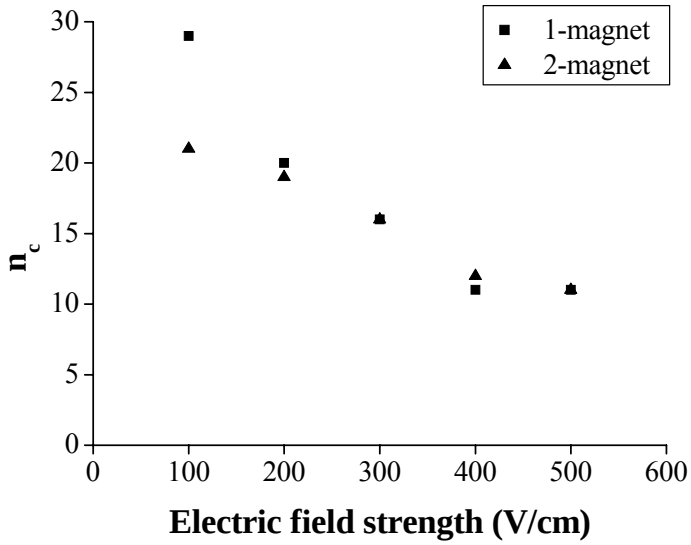

Figure 2.8. Effect of electric field strength on peak capacity (n_c) for assays of alkaline phosphatase inhibition by arsenate. Experimental conditions are the same as in Figure 2.5, except that the electric field strength was varied as indicated. The electric field strength for each arsenate injections matched the separation field strength for that experiment.

The results of inhibition assays (arsenate, alkaline phosphatase) with different bead injection times using both microreactor configurations are presented in Figure 2.9. Increasing the bead injection time increases the total number of beads injected and the bead plug length (Figure 2.10). The image of a bead plug at bead injection time of 15 s for the 2-magnet configuration is shown in Figure 2.10. The density of magnetic beads in a plug is difficult to be determined from 2-D images of the 3-D system.

Figure 2.9a shows a plot of peak capacity as the bead injection time is increased from 3.0 s to 90 s. For both magnet configurations, the peak capacity decreases dramatically when the bead injection time is increased from 15 to 30 s. There appears to be a slight increasing trend in peak capacity as the injection time is increased from 30 to 90 s. The peak capacity is proportional to the ratio of the migration time (t) over the peak width ($w_{1/2}$). For inhibition assays by arsenate, the migration time of the inhibitor does not change much at different bead injection times. The

trend of peak capacity vs. bead injection time results mainly from the variation of the inhibition peak width. The inhibition peak width for inhibition assays using enzyme microreactors with magnetic beads is a complicated and interesting issue, and the cause of the inhibition peak broadening is not yet clearly and completely understood. In this study, our focus is put on improving the peak capacity for inhibitor separations.

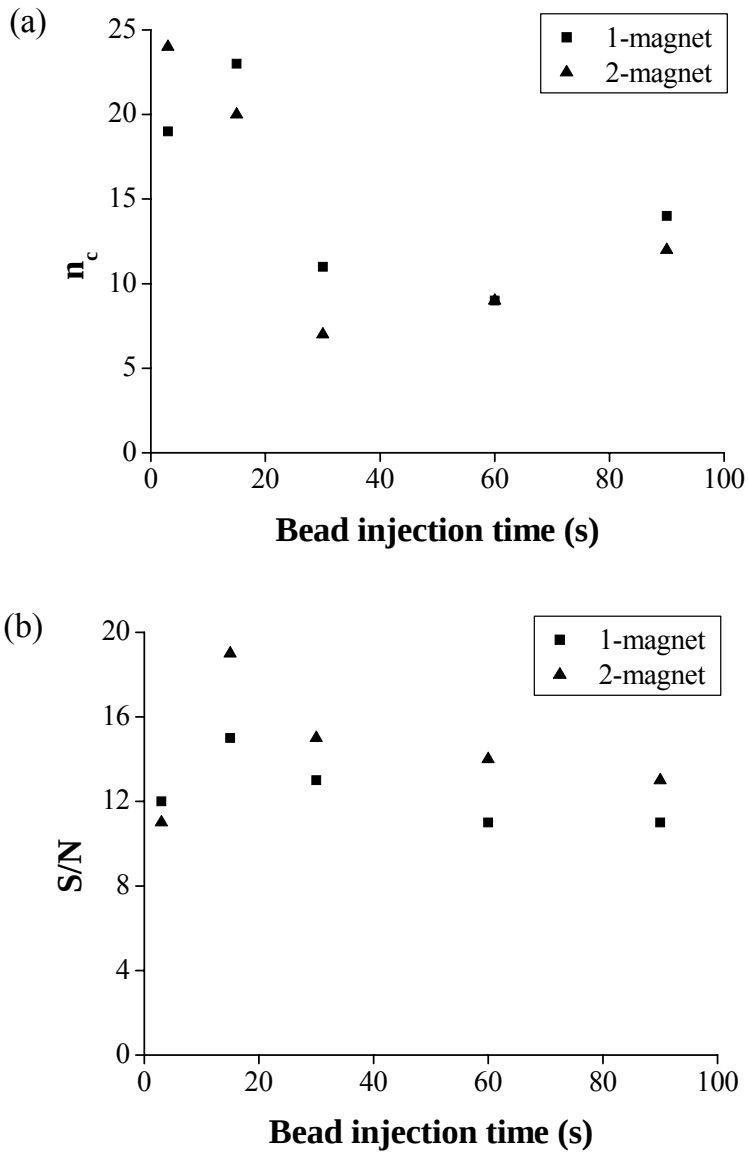

Figure 2.9. Effect of bead injection time on (a) peak capacity (n_c) and (b) inhibition peak S/N for assays of alkaline phosphatase inhibition by arsenate. Experimental conditions are the same as in Figure 2.5, except that bead injection time was varied as indicated.

The increase in bead injection time also affects the S/N for the inhibition peaks for both enzyme microreactor types as shown in Figure 2.9b. The fluorescence signal due to enzyme-catalyzed product formation increases as the number of beads immobilized increases due to increased bead injection time. With longer magnetic bead injection time, the inhibition peak height increases; however, the baseline noise also increases. The S/N of the inhibition peak only changes slightly for the bead injection times investigated here. A magnetic bead injection time of 15.0 s was used for later experiments to obtain an enhanced peak capacity ($n_c \approx 20$) and S/N.

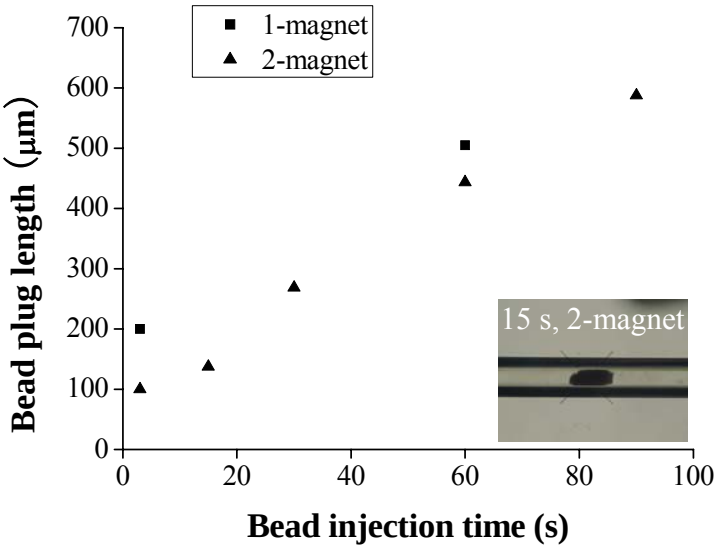

Figure 2.10. Effect of bead injection time on bead plug length. Magnetic beads (1.7×10^8 beads/mL) coated with alkaline phosphatase in DEA buffer (50.00 mM, pH 9.50) were injected at 300 V/cm for different time periods. Then, the beads were transported to the immobilizing magnets at 300 V/cm for the 1-magnet configuration and 200 V/cm for the 2-magnet configuration.

Inhibition of alkaline phosphatase by theophylline with different magnetic bead injection times also was studied for both magnet configurations. These results are shown in Figure 2.11. The peak capacity for theophylline is less impacted by the bead injection time compared to

arsenate, ranging only from 17-25 for all bead injection times and both enzyme microreactor configurations. The S/N increases for theophylline by approximately a factor of two for both magnet configurations when the bead injection time is increased from 3.0 to 15 s. At longer bead injection times, the S/N ratio is relatively stable as was observed for arsenate inhibition.

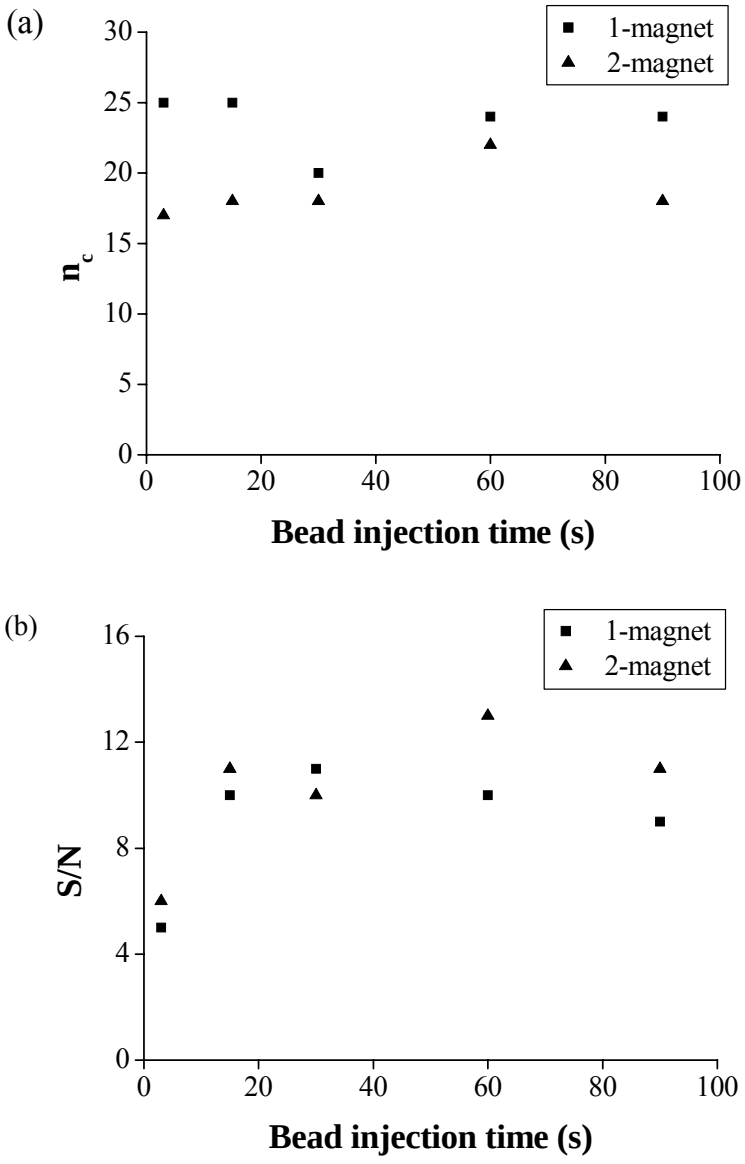

Figure 2.11. Effect of bead injection time on (a) peak capacity (n_c) and (b) inhibition peak S/N for assays of alkaline phosphatase inhibition by theophylline. Experimental conditions are the same as in Figure 2.7, except that bead injection time was varied as indicated.

2.3.5 Inhibition Peak Shape and Inhibitor Concentration

To investigate the effect of inhibitor concentration on inhibition peak shape, different concentrations of sodium arsenate were injected for 3.0 s using both 1 and 2-magnet enzyme microreactors. Figure 2.12 shows electropherograms for inhibition assays at different arsenate concentrations using a 1-magnet enzyme microreactor. The electropherograms are artificially offset vertically to more clearly show the inhibition peaks, but the fluorescence baselines were the same in the original electropherograms. The artifact peaks at ~5.0 min are about the same for assays at lower arsenate concentrations, and get deeper and wider at arsenate concentration of 12.5 mM. The positive peaks at ~8.9 min are for fluorescein, which was used as a control since it is not expected to interact with the immobilized enzyme and magnetic beads. The inhibition peaks become deeper and broader as the inhibitor concentration increases. Plots of the inhibition peak width at half maximum ($w_{1/2}$) vs. the inhibitor concentration (Figure 2.13) for both enzyme microreactor types show that the peak widths increase by more than a factor of 20 in both cases. The fluorescein peaks have similar peak width for both magnet configurations. The fluorescein peak widths are ~ 0.04 min at inhibitor concentrations from 0.0125 mM to 1.25 mM, and decrease to 0.01 min due to sample stacking effect at inhibitor concentration of 12.5 mM. It is proved by the narrowness of fluorescein peaks that fluorescein does not interact with the enzyme coated on magnetic beads. Furthermore, the large widths of inhibition peaks should result from the interaction between inhibitor and enzyme when the inhibitor migrates passing the bead plug.

The effect of inhibitor concentration on inhibition peak shape was also studied for theophylline using both enzyme microreactors. The electropherograms for these experiments with a 1-magnet microreactor are presented in Figure 2.14. Theophylline inhibition was also studied using the EMMA method previously reported by Whisnant et al. [50, 51]. The

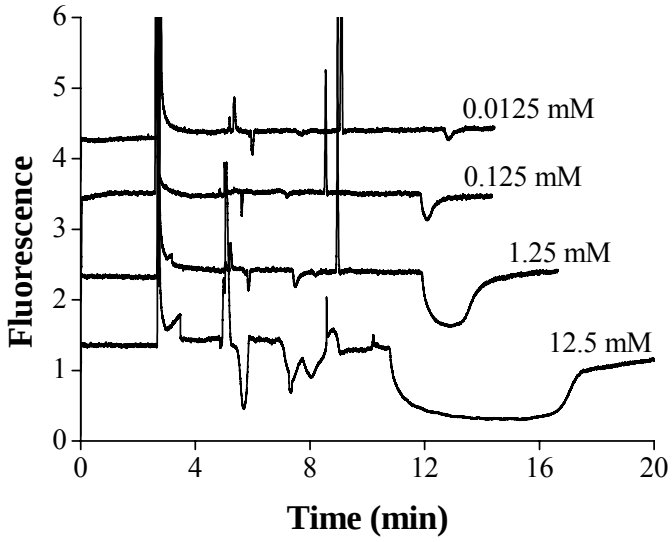

Figure 2.12. Electropherogram of enzyme inhibition assays at different arsenate concentrations using an enzyme microreactor constructed with a single magnet. Magnetic beads (1.7×10^8 beads/mL) were injected for 15.0 s at 18.0 kV. A mixture of 0.5 μM fluorescein and the inhibitor, arsenate, was injected for 3.0 s at 12.0 kV, and then the separation potential of 12.0 kV was applied. All other experimental conditions are the same as in Figure 2.5. The electropherograms were artificially offset along the vertical axis so the inhibition peaks could be viewed without overlap.

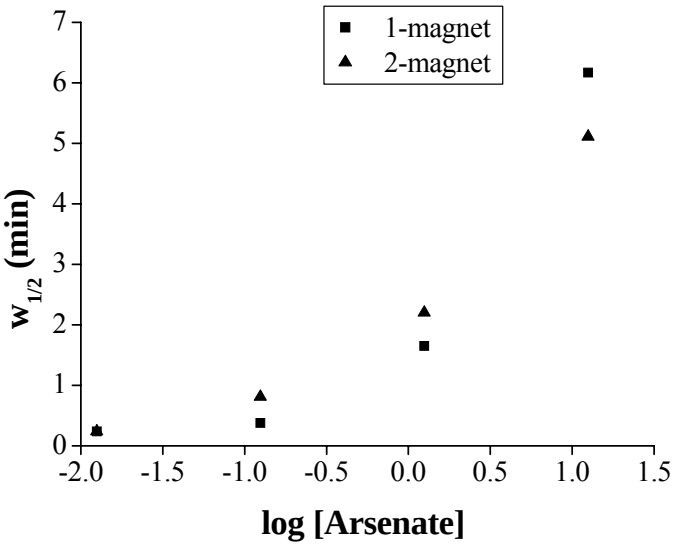

Figure 2.13. Plots of inhibition peak width at half maximum ($w_{1/2}$) vs. inhibitor concentration for assays of alkaline phosphatase inhibition by arsenate. Experimental conditions are the same as in Figure 2.12.

electropherograms for the EMMA studies are presented in Figure 2.15. Figure 2.16 shows plots of the inhibition peak widths at half maximum ($w_{1/2}$) vs. theophylline concentration for all three assays. For all three assays the peak width increases by a factor of 6 as the theophylline concentration increases from 0.500 to 10.0 mM. At all inhibitor concentrations, the inhibition peak width for heterogeneous assays is 40-110% larger than that for the homogeneous assay. For both heterogeneous assays and homogeneous assays, the inhibition peak width is not the physical length of the inhibitor plug. For heterogeneous assays, a major contribution to the inhibition peak width comes from the interaction between the inhibitor and the enzyme on magnetic beads. For homogeneous assays, the electrophoretic mobilities of the enzyme and inhibitor plugs and also the interaction between these two plugs determine the inhibition peak width.

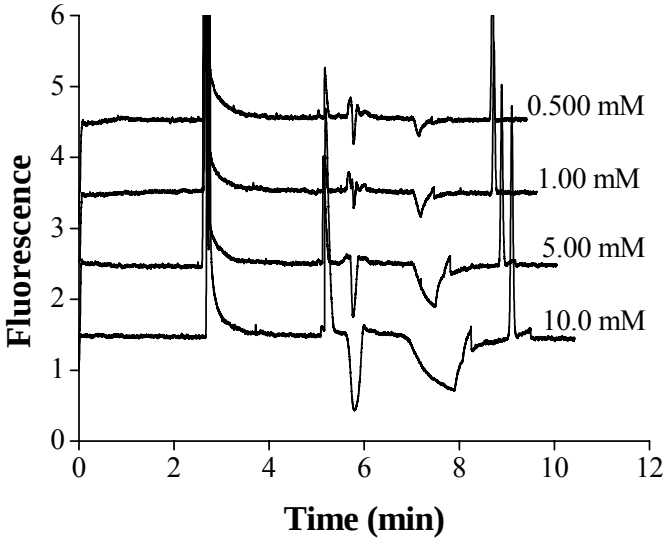

Figure 2.14. Electropherogram of enzyme inhibition assays using an enzyme microreactor constructed with a single magnet at different theophylline concentrations. Magnetic beads (1.7×10^8 beads/mL) were injected for 15.0 s at 18.0 kV. A mixture of 0.5 μM fluorescein and the inhibitor, theophylline, was injected for 3.0 s at 12.0 kV, and then the separation potential of 12.0 kV was applied. All other experimental conditions are the same as in Figure 2.7. The electropherograms were artificially offset along the vertical axis so the inhibition peaks could be viewed without overlap.

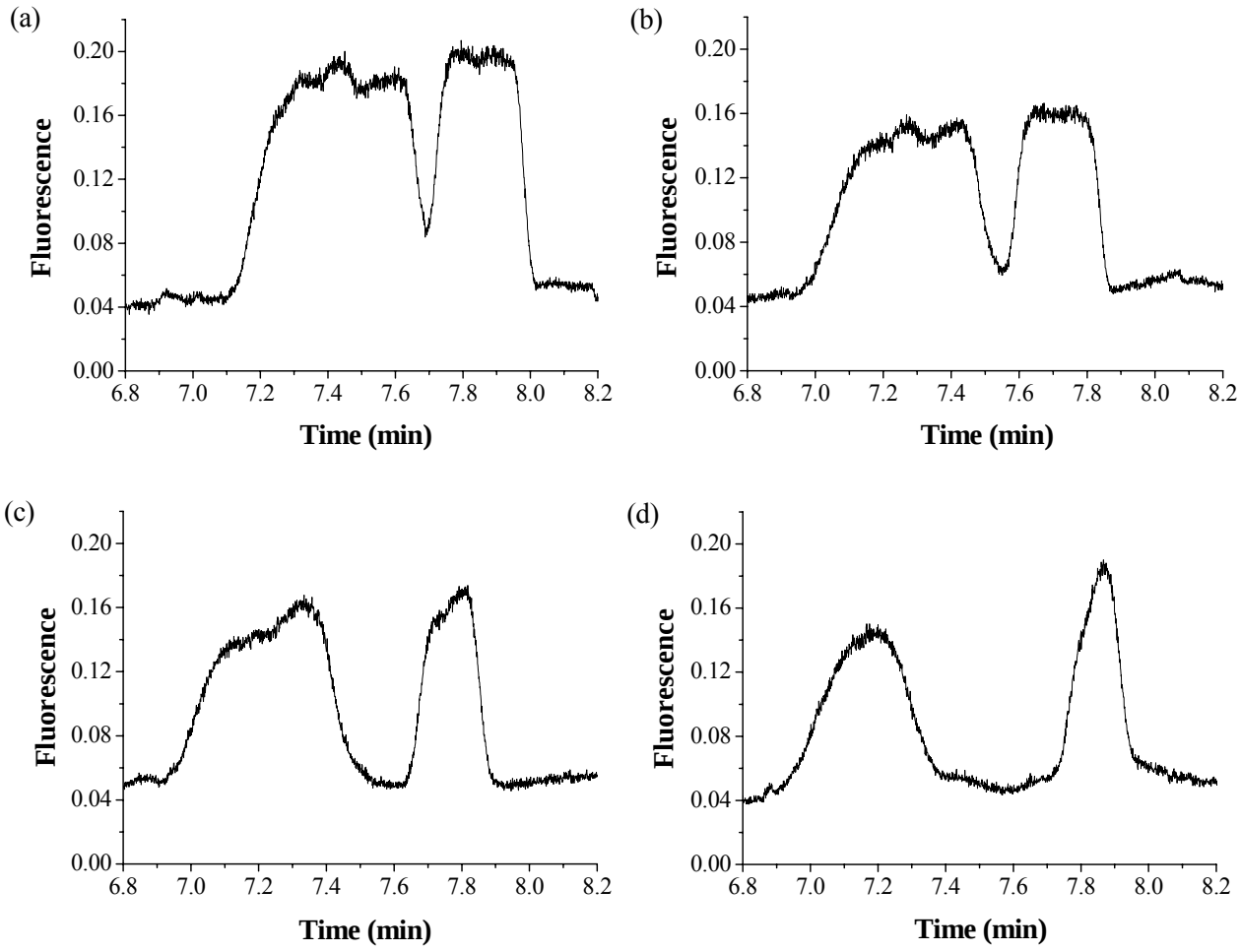

Figure 2.15. Electropherograms of enzyme inhibition assays using homogeneous EMMA at different theophylline concentrations. (a) 0.500 mM; (b) 1.00 mM; (c) 5.00 mM; (d) 10.0 mM. A plug of the inhibitor, theophylline, was injected for 3.0 s at 12.0 kV into a capillary filled with 0.100 mM AttoPhos (50.00 mM DEA, pH 9.50). Next, a potential of 12.0 kV was applied for 30.0 s. Then, a plug of 51 pM alkaline phosphatase was injected into the capillary for 3.0 s at 12.0 kV. Finally, a separation potential of 12.0 kV (200 V/cm) was

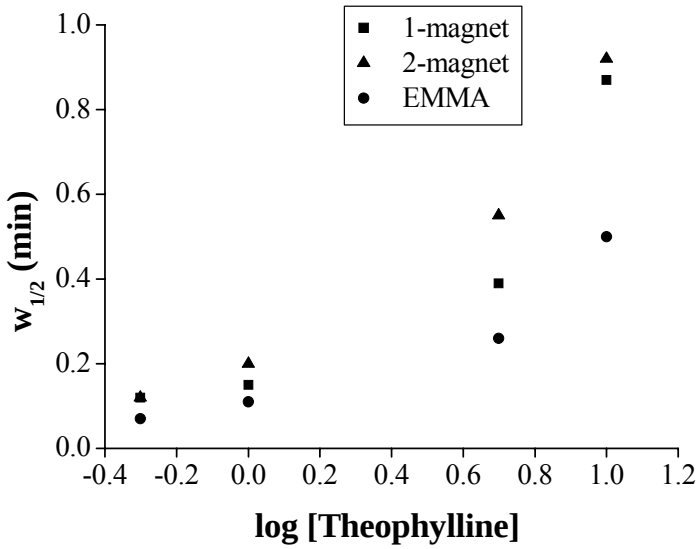

Figure 2.16. Plots of inhibition peak width at half maximum ($w_{1/2}$) vs. inhibitor concentration for assays of alkaline phosphatae inhibition by theophylline. Experimental conditions for heterogeneous assays using enzyme microreactors are the same as in Figure 2.14. Experimental conditions for homogeneous assays based on EMMA are the same as in Figure 2.15.

2.3.6 Separation and Detection of Enzyme Inhibitor Mixtures

Figure 2.17 presents a separation of a mixture of 5 inhibitors of alkaline phosphatase using a 1-magnet enzyme microreactor. The inhibitors were electrophoretically separated in the capillary before reaching the enzyme microreactor, and the inhibitor zones produced negative peaks due to reduced product formation as they passed through the enzyme microreactor. All 5 analytes, tryptophan, theophylline, vanadate, arsenate and tungstate, are reversible inhibitors of alkaline phosphatase [57-60]. The same experiment was performed with a 2-magnet enzyme microreactor (Figure 2.18). All 5 inhibitors as well as fluorescein (peak 6) were resolved from each other and from artifact peaks in both experiments. Inhibition assays of the five species also were carried out individually so that the inhibition peaks could be identified according to their migration times (data not shown).

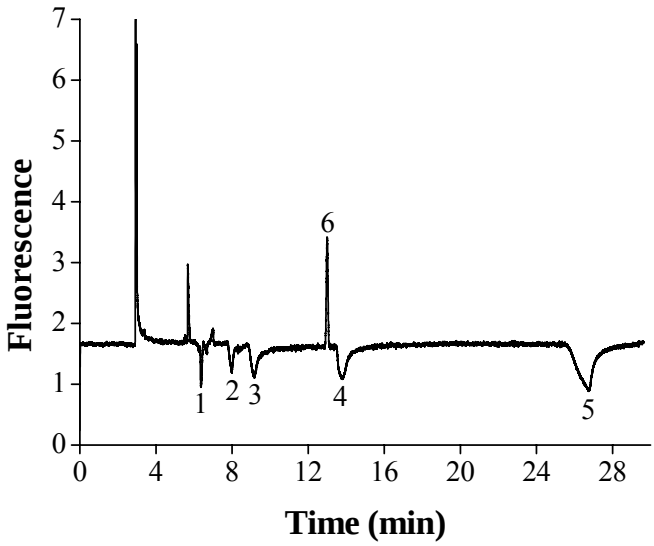

Figure 2.17. Separation of alkaline phosphatase inhibitors using a 1-magnet enzyme microreactor. Peak identities are: 1. tryptophan; 2. theophylline; 3. sodium vanadate; 4. sodium arsenate; 5. sodium tungstate; 6. fluorescein. Magnetic beads (1.7×10^8 beads/mL) were injected for 15.0 s at 18.0 kV (300 V/cm). A mixture of five inhibitors was injected for 3.0 s at 12.0 kV (200 V/cm). Other experimental conditions are the same as in Figure 2.5.

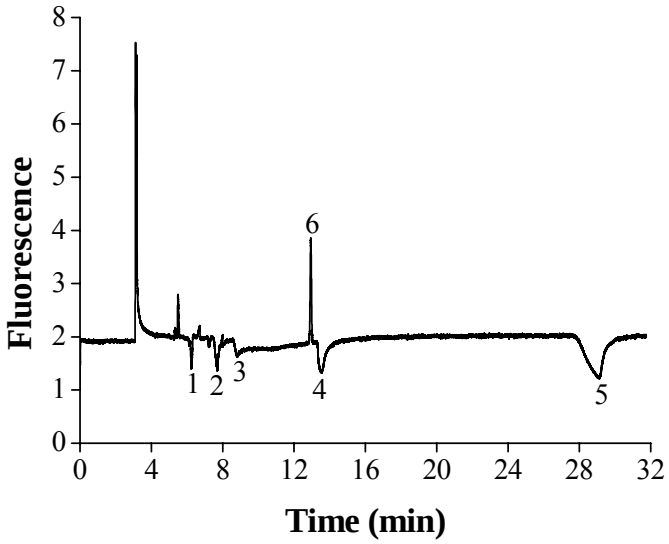

Figure 2.18. Separation of alkaline phosphatase inhibitors using a 2-magnet enzyme microreactor. Peak identities are: 1. tryptophan; 2. theophylline; 3. sodium vanadate; 4. sodium arsenate; 5. sodium tungstate; 6. fluorescein. Experimental conditions are the same as in Figure 2.17.

The same separation was attempted using the homogeneous method combining continuous EMMA and transient engagement EMMA [50, 51]. The result of this experiment is presented in Figure 2.19. Only two peaks are apparent in the product plateau in the electropherogram from 6.2 to 7.0 min. Based on the migration order of the inhibitors from the experiments in Figures 2.17 and 2.18 as well as experiments using the homogeneous EMMA method in which the samples were spiked with arsenate or tryptophan, these peaks were identified as theophylline (6.5 min) and vanadate (6.8 min). The product plateau was so narrow that the inhibition peaks for tryptophan, arsenate and tungstate were not observed. Tryptophan migrated fastest among the five inhibitors, and its migration time should be less than 6.2 min. Arsenate had a lower electrophoretic mobility than vanadate. Tungstate moved slowest. Arsenate and tungstate peaks should be on the right edge of the product plateau. These results show that the homogeneous EMMA method has very limited peak capacity, and in this case it cannot separate and detect all five inhibitors of alkaline phosphatase.

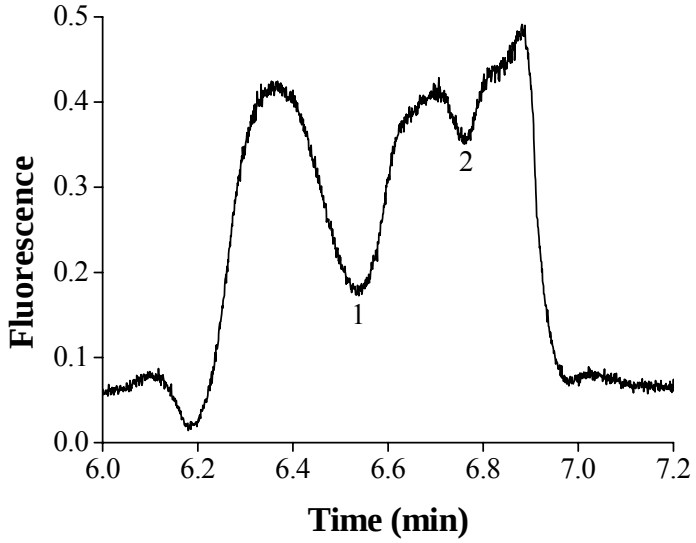

Figure 2.19. Separation of alkaline phosphatase inhibitors using homogeneous EMMA. Peak identities are: 1. theophylline; 2. sodium vanadate. A mixture of five alkaline phosphatase inhibitors was injected for 3.0 s at 12.0 kV into a capillary filled with 0.100 mM AttoPhos (50.00 mM DEA, pH 9.50). Next, a potential of 12.0 kV was applied for 40.0 s. Then, a plug of 51.0 pM alkaline phosphatase was injected into the capillary for 3.0 s at 12.0 kV. Finally, a separation potential of 12.0 kV (200 V/cm) was applied.

CHAPTER 3
CONCLUSIONS AND FUTURE DIRECTIONS

3.1 Conclusions

An on-column enzyme microreactor was created for electrophoretic separations and detection of enzyme inhibitors by immobilizing an enzyme (alkaline phosphatase) inside a capillary using magnetic beads. Enzyme inhibition assays were performed together with inhibitor separations in a single run. A fluorogenic substrate, AttoPhos, was included in the running buffer for the assays. Product was generated in the enzyme microreactor and detected by laser-induced fluorescence. Enzyme inhibition by each separated inhibitor species could be observed as a negative peak due to decreased product formation. Using this approach, the peak capacity for inhibitor separations was greatly enhanced compared to previous studies employing a method combing continuous engagement EMMA and transient engagement EMMA [50, 51].

To construct the on-column enzyme microreactor, alkaline phosphatase-coated superparamagnetic beads were eletrophoretically injected into the capillary and then transported by electrophoresis to the immobilizing magnet(s) at the downstream end of the capillary before the detection window. Two different magnet configurations, a single B442 magnet and a pair of D24 magnets, were used in this study. In both configurations, the magnetic field was sufficiently strong that magnetic beads were held in place successfully inside the capillary. The one-magnet configuration provided a higher peak capacity for separations of enzyme inhibitors. Therefore, the use of one-magnet configuration was preferred. A significant advantage of the approach for enzyme microreactor construction developed in this thesis is that the capillary can be reused by simply rinsing out the magnetic beads using a manual syringe pump.

The goal of this study was to increase the peak capacity (n_c) for inhibitor separations relative to previous work [50, 51] while performing detection based on enzyme inhibition. The effects of

the applied field strength and bead injection time on peak capacity were investigated. Generally, the peak capacity decreased with increasing field strength for both magnet configurations. Considering both peak capacity and time required for electrophoretic separation, a field strength of 200 V/cm with $n_c \approx 20$ was chosen for later experiments. The bead injection time determines the number of alkaline phosphatase-coated magnetic beads injected and the length of the resulting bead plug. For alkaline phosphatase inhibition assays with arsenate (reversible, competitive inhibitor), the peak capacity first decreased rapidly as the bead injection time increased from 15 to 30 s. The peak capacity then increased slowly when bead injection time was increased further. Moreover, the S/N of arsenate inhibition peak did not change significantly for different bead injection times. For inhibition assays with theophylline (reversible, noncompetitive inhibitor), changing bead injection time had less of an effect on the peak capacity compared to arsenate. The S/N of theophylline inhibition peak was low with bead injection time of 3.0 s, and then increased by approximately a factor of 2 when the bead injection time was increased to 15 s. At longer bead injection times, the S/N ratio was relatively stable. Considering both the peak capacity and S/N, a magnetic bead injection time of 15.0 s was used for later experiments ($n_c \approx 20$).

The effect of inhibitor concentration on inhibition peak width at half maximum ($w_{1/2}$) also was studied. For inhibition assays with arsenate and assays with theophylline, the inhibition peak width increased with inhibitor concentration. For heterogeneous assays with arsenate using both one-magnet and two-magnet enzyme microreactors, the inhibition peak width increased by more than a factor of 20. For heterogeneous assays with theophylline using both enzyme microreactors and homogeneous assays with theophylline using the EMMA method, the inhibition peak width

increased by a factor of 6. Moreover, at all theophylline concentrations, the inhibition peak width for heterogeneous assays was 40-110% larger than that for homogeneous assays.

A separation of five reversible inhibitors of alkaline phosphatase (theophylline, vanadate, arsenate, L-tryptophan and tungstate) was demonstrated using both the one and two-magnet enzyme microreactors. The inhibitors were separated by capillary electrophoresis before reaching the enzyme microreactor. All of the five inhibitors were baseline resolved within 30 min. A peak capacity (n_c) of 22 was obtained. The high separation efficiency of capillary electrophoresis provides this method the potential to screen enzyme inhibitors in a complex mixture.

Homogeneous inhibition assays of alkaline phosphatase with a mixture of the five inhibitors also were carried out using a method developed previously in our lab [50, 51] which combines continuous engagement EMMA and transient engagement EMMA. Using this EMMA method, at most three inhibition peaks could be observed. The peak capacity for this method was shown to be very limited compared to our new approach using enzyme microreactors with magnetic beads.

3.2 Future Studies

Future studies based on the research in this thesis will focus on developing other novel approaches for separations of mixtures of enzyme inhibitors using on-line enzyme inhibition assays based on CE. Priority will still be placed on increasing the peak capacity for inhibitor separations. In preliminary work, an approach of carrying out temperature-controlled enzyme-catalyzed reactions in a capillary was employed for enzyme inhibitor separations. The idea was to separate enzyme inhibitors when the enzyme activity was suppressed at a very low temperature and to detect negative inhibition peaks of individual inhibitors by initiating the

enzyme-catalyzed reaction at a high temperature. Two enzymes, alkaline phosphatase and horseradish peroxidase, were used in this approach, but the difference of enzyme activity at different temperatures was not great enough for this approach to succeed.

One promising strategy for performing CE separations of enzyme inhibitors together with enzyme inhibition assays is to use liposomes to encapsulate substrate or enzyme. In this approach the capillary would be filled first with enzyme and its fluorogenic substrate which will be contained in liposomes. The interaction between enzyme and substrate would be blocked by the lipid membrane. A zone of inhibitor mixtures would be injected into the capillary. Inhibitors would be separated electrophoretically. After the separations of inhibitors, free substrate would be released from liposomes in the capillary by photolysis or electrochemical reactions to develop the enzyme-catalyzed reaction. Product generation would be observed as a constant fluorescence signal. Separated inhibitors would interact with the enzyme-substrate complex, and their respective negative peaks would be detected. Preliminary work to synthesize photolabile liposomes was carried out but not completed.

Another approach for performing inhibitor separations and enzyme inhibition assays by CE would be using caged compounds. This approach is similar to the approach using liposomes in that the enzyme-catalyzed reaction is first blocked and then triggered to occur by an external stimulation. In this approach, enzyme substrate or cofactor would be modified chemically with a photolabile protecting group. Inhibitor mixtures would be separated first in a capillary filled with enzyme and substrate or cofactor which is protected by the caging group. Upon photolysis in the capillary, the protecting group of the caged enzyme substrate or cofactor would be removed to develop the enzyme-catalyzed reaction. Separated inhibitors would be detected as individual negative peaks due to enzyme inhibition.

REFERENCES

[1] Berg, J. M., Tymoczko, J. L., Stryer, L., *Biochemistry*, Freeman Press, New York 2002.

[2] Eisenthal, R., Danson, M. J., *Enzyme assays: A practical approach*, Oxford University Press, Oxford 1992.

[3] Bugg, T., *Introduction to enzyme and coenzyme chemistry*, Blackwell Publishing, Malden 2004.

[4] Copeland, R. A., *Enzymes : A practical introduction to structure, mechanism, and data analysis* Wiley & Sons, New York 2000.

[5] Leskovac, V., *Comprehensive enzyme kinetics*, Kluwer Academic/Plenum Publishers, New York 2003.

[6] Marangoni, A. G., *Enzyme kinetics: A modern approach* Wiley & Sons, Hoboken 2003.

[7] Copeland, R. A., *Evaluation of enzyme inhibitors in drug discovery: A guide for medicinal chemists and pharmacologists*, Wiley & Sons, Hoboken 2005.

[8] Schafer, T., Borchert, T. W., Nielsen, V. S., Skagerlind, P., *et al.*, *Adv. Biochem. Eng./Biotechnol.* 2007, *105*, 59-131.

[9] Tzanov, T., Andreaus, J., Guebitz, G., Cavaco-Paulo, A., *Electron. J. Biotechnol.* 2003, *6*, 146-154.

[10] Thanikaivelan, P., Rao, J. R., Nair, B. U., Ramasami, T., *Trends Biotechnol.* 2004, *22*, 181-188.

[11] Maurer, K.-H., *Curr. Opin. Biotechnol.* 2004, *15*, 330-334.

[12] Sjoede, A., Winestrand, S., Nilvebrant, N.-O., Joensson, L. J., *Enzyme Microb. Technol.* 2008, *43*, 78-83.

[13] Merino, S. T., Cherry, J., *Adv. Biochem. Eng./Biotechnol.* 2007, *108*, 95-120.

[14] Davis, B. G., Boyer, V., *Nat. Prod. Rep.* 2001, *18*, 618-640.

[15] Azevedo, A. M., Prazeres, D. M. F., Cabral, J. M. S., Fonseca, L. P., *Biosens. Bioelectron.* 2005, *21*, 235-247.

[16] Perez, J. P. H., Lopez-Cabarcos, E., Lopez-Ruiz, B., *Biomol. Eng.* 2006, *23*, 233-245.

[17] Giddings, J. C., *Unified separation science*, Wiley & Sons, New York 1991.

[18] Landers, J. P., *Handbook of capillary and microchip electrophoresis and associated microtechniques*, CRC Press, Boca Raton 2008.

[19] Regnier, F. E., Patterson, D. H., Harmon, B. J., *Trends in Analytical Chemistry* 1995, *14*, 177-181.

[20] Bao, J. J., Fujima, J. M., Danielson, N. D., *Journal of Chromatography B: Biomedical Sciences and Applications* 1997, *699*, 481-497.

[21] Van Dyck, S., Kaale, E., Novakova, S., Glatz, Z., *et al.*, *Electrophoresis* 2003, *24*, 3868-3878.

[22] Novakova, S., Van Dyck, S., Van Schepdael, A., Hoogmartens, J., Glatz, Z., *Journal of Chromatography A* 2004, *1032*, 173-184.

[23] Zhang, J., Hoogmartens, J., Van Schepdael, A., *Electrophoresis* 2006, *27*, 35-43.

[24] Glatz, Z., *Journal of Chromatography B: Analytical Technologies in the Biomedical and Life Sciences* 2006, *841*, 23-37.

[25] Zhang, J., Hoogmartens, J., Van Schepdael, A., *Electrophoresis* 2008, *29*, 56-65.

[26] Krenkova, J., Foret, F., *Electrophoresis* 2004, *25*, 3550-3563.

[27] Bao, J., Regnier, F. E., *Journal of Chromatography* 1992, *608*, 217-224.

[28] Chantiwas, R., Yan, X., Gilman, S. D., in: Gomez, F. A. (Ed.), *Biological applications of microfluidics*, Wiley & Sons, Hoboken 2008, pp. 135-170.

[29] Burke, B. J., Regnier, F. E., *Electrophoresis* 2001, *22*, 3744-3751.

[30] Kanie, Y., Kanie, O., *Carbohydr. Res.* 2002, *337*, 1757-1762.

[31] Sun, X., Jin, W., *Anal. Chem.* 2003, *75*, 6050-6055.

[32] Sun, X., Jin, W., Li, D., Bai, Z., *Electrophoresis* 2004, *25*, 1860-1866.

[33] Novakova, S., Van Dyck, S., Glatz, Z., Van Schepdael, A., Hoogmartens, J., *Journal of Chromatography A* 2004, *1032*, 319-326.

[34] Green, J. M., *Weed Technol.* 2007, *21*, 547-558.

[35] Zhou, Q., Liu, W., Zhang, Y., Liu, K. K., *Pestic. Biochem. Physiol.* 2007, *89*, 89-96.

[36] Pope, C. N., *J Toxicol Environ Health B Crit Rev* 1999, *2*, 161-181.

[37] Poet, T. S., Kousba, A. A., Dennison, S. L., Timchalk, C., *Neurotoxicology* 2004, *25*, 1013-1030.

[38] Ouaissi, M., Ouaissi, A., *J. Biomed. Biotechnol.* 2006, 13474-13483.

[39] Sakai-Kato, K., Kato, M., Toyo'oka, T., *Journal of Chromatography A* 2004, *1051*, 261-266.

[40] Tang, Z.-M., Kang, J.-W., *Anal. Chem.* 2006, *78*, 2514-2520.

[41] Park, S.-S., Cho Seung, I., Kim, M.-S., Kim, Y.-K., Kim, B.-G., *Electrophoresis* 2003, *24*, 200-206.

[42] Belenky, A., Hughes, D., Korneev, A., Dunayevskiy, Y., *Journal of Chromatography A* 2004, *1053*, 247-251.

[43] Hadd, A. G., Raymond, D. E., Halliwell, J. W., Jacobson, S. C., Ramsey, J. M., *Anal. Chem.* 1997, *69*, 3407-3412.

[44] Saevels, J., Van den Steen, K., Van Schepdael, A., Hoogmartens, J., *Journal of Chromatography A* 1996, *745*, 293-298.

[45] Novakova, S., Telnarova, M., Glatz, Z., *Journal of Chromatography A* 2003, *990*, 189-195.

[46] Telnarova, M., Vytiskova, S., Monincova, M., Glatz, Z., *Electrophoresis* 2004, *25*, 1028-1033.

[47] Papezova, K., Nemec, T., Chaloupkova, R., Glatz, Z., *Journal of Chromatography A* 2007, *1150*.

[48] Iqbal, J., Burbiel, J. C., Mueller, C. E., *Electrophoresis* 2006, *27*, 2505-2517.

[49] Van Dyck, S., Van Schepdael, A., Hoogmartens, J., *Electrophoresis* 2001, *22*, 1436-1442.

[50] Whisnant, A. R., Johnston, S. E., Gilman, S. D., *Electrophoresis* 2000, *21*, 1341-1348.

[51] Whisnant, A. R., Gilman, S. D., *Analytical Biochemistry* 2002, *307*, 226-234.

[52] Hadd, A. G., Jacobson, S. C., Ramsey, J. M., *Anal. Chem.* 1999, *71*, 5206-5212.

[53] Rashkovetsky, L. G., Lyubarskaya, Y. V., Foret, F., Hughes, D. E., Karger, B. L., *Journal of Chromatography A* 1997, *781*, 197-204.

[54] Slovakova, M., Minc, N., Bilkova, Z., Smadja, C., *et al.*, *Lab Chip* 2005, *5*, 935-942.

[55] Chetwyn, N. P., *Department of Pharmaceutical Chemistry*, University of Kansas, Lawrence, KS 1997, p. 400.

[56] Lacey, M. E., Webb, A. G., Sweedler, J. V., *Anal. Chem.* 2000, *72*, 4991-4998.

[57] Bublitz, R., Armestoz, J., Hoffmann-Blume, E., Schljlze, M.*, et al.*, *European Journal of Biochemistry* 1993, *217*, 199-207.

[58] Farley, J. R., hey, J. L., Baylink, D. J., *The Journal of Biological Chemistry* 1980, *255*, 4680-4686.

[59] O'Brie, P. J., Herschlag, D., *Biochemistry* 2002, *41*, 3207-3225.

[60] Shirazi, S. P., Beechey, R. B., Butterworth, P. J., *Biochemistry Journal* 1981, *194*, 803-809.

VITA

Xiaoyan Yan was born in November 1978 in Rongcheng, Shandong Province, China. In 1990, her family moved to Dalian, Liaoning Province, China. She enrolled in Dalian University of Technology, Dalian, China, in 1996. From Dalian University of Technology, she earned her Bachelor of Science degree in chemical engineering in 2001. She then attended Dalian Institute of Chemical Physics, Chinese Academy of Sciences, Dalian, China, for three years. In January 2005, she enrolled in Louisiana State University to study analytical chemistry.